Behavioural Brain Research 210 (2010) 211–220

Contents lists available at ScienceDirect

Behavioural Brain Research

journal homepage: www.elsevier.com/locate/bbr

Research report

The role of the estrogen receptor α in the medial amygdala and ventromedial nucleus of the hypothalamus in social recognition, anxiety and aggression

Thierry Spiteri[a], Sergei Musatov[b,c,d], Sonoko Ogawa[e], Ana Ribeiro[b], Donald W. Pfaff[b], Anders Ågmo[a,*]

[a] Department of Psychology, University of Tromsø, 9037 Tromsø, Norway
[b] Laboratory of Neurobiology and Behavior, The Rockefeller University, New York, NY 10021, United States
[c] Neurologix Inc., Fort Lee, NJ 07024, United States
[d] Laboratory of Molecular Neurosurgery, Weill Medical College of Cornell University, New York, NY 10021, United States
[e] Laboratory of Behavioral Neuroendocrinology, University of Tsukuba, Tsukuba, Japan

ARTICLE INFO

Article history:
Received 11 January 2010
Received in revised form 16 February 2010
Accepted 17 February 2010
Available online 23 February 2010

Keywords:
Social recognition
Anxiety
Aggressiveness
Estrogen receptor α
Medial posterodorsal amygdala
Ventromedial nucleus of the hypothalamus

ABSTRACT

Social recognition manifests itself in decreased investigation of a previously encountered individual. Estrogen receptor alpha (ERα) knock out mice show deficient social recognition and anxiety. These data show that the ERα is involved in these effects, but they do not say anything about the brain sites important for these effects. In this study, an shRNA encoded within an AAV viral vector directed against the ERα receptor gene (or containing luciferase control), was injected bilaterally into the posterodorsal amygdala (MePDA) or the ventromedial nucleus of the hypothalamus (VMN) of female rats. An 81% reduction of ERα expression in the MePDA eliminated social recognition. Moreover, this diminution of ERα in the MePDA reduced anxiety in the light/dark choice test. In contrast, social recognition was unaffected after ERα knockdown in the VMN while aggressiveness against the juvenile was enhanced. In conclusion, social recognition and anxiety in female rats are modulated by the ERα in the amygdala. Moreover, aggression against juveniles but not against adults could, at least partly, depend on the ERα in the VMN.

1. Introduction

During the last decade the interest in the estrogenic regulation of behavioral processes beyond sexual behaviors has increased hugely. Estrogens have been shown to be implicated in cognitive functions [48], emotional reactions such as anxiety and fear [54] and social behaviors [80]. The role of estrogens in social recognition has also attracted some attention.

Social recognition is the ability to recognize familiar conspecifics and manifests itself in decreased investigation of a previously encountered individual [75]. The estrogenic regulation of social recognition in rodents has been investigated in a few studies with inconsistent results [30,47,64,74]. Nevertheless, a recent study showed that estradiol + progesterone improved social recognition in female rats [70]. A study in female mice, whose gene for the estrogen receptor alpha (ERα) or the estrogen receptor β (ERβ) had been knocked out, showed that they were deficient in social recognition compared to the wildtype [13]. Thus, there are data implicating ERs in social recognition, but these data gives no clue as to which of the ERs that is involved nor to the important brain site. Since there is ample evidence showing that the medial amygdala is important for social recognition [11,14,19], as well as being a structure where ERs are abundant [58], it is conceivable that estrogen actions within this structure are involved social recognition.

Anxiety is prominent among the emotions in which estrogens have been implicated. However, experimental results range from anxiogenic [29,35,53] to anxiolytic [35,46,59,78,82], and some studies report no effects at all [20,51,56]. The contradictory data could perhaps be explained by opposing actions of estradiol on the ERα and ERβ. Indeed, there are much recent data suggesting that stimulation of the ERβ consistently has anxiolytic effects [32,45,77]. It has also been proposed that estrogens are anxiolytic in safe environments, thereby facilitating sexual behaviors, and anxiogenic in threatening environments [54]. There is, then, no doubt that estrogens may exert important influences on anxiety-related behaviors. Whether the action is anxiolytic or anxiogenic may depend both on the environment and on the receptor subtype activated.

The medial amygdala is a crucial structure for emotional responses related to fear and anxiety [3,52,63]. Injection of estradiol into the medial amygdala has anxiolytic effects similar to those observed after systemic estradiol administration [23]. This observation suggests that the medial amygdala is an important target for the anxiolytic effects of estrogens. However the implication of ERα in this process remains to be demonstrated.

* Corresponding author. Tel.: +47 77 64 63 65; fax: +47 77 64 52 91.
E-mail address: anders.agmo@uit.no (A. Ågmo).

0166-4328/$ – see front matter © 2010 Elsevier B.V. All rights reserved.
doi:10.1016/j.bbr.2010.02.033

The VMN may also be involved in the control of anxiety [26,49,67]. Whether estrogen receptors are involved in these actions is unknown, but since estrogens are known to modify the excitability of at least some neurons in the VMN [38,39,81] this is a definite possibility.

Another behavior modified by estrogens is aggression. In female rats as well as in mice it seems that estrogens increase aggression in some cases while estrogen + progesterone may reduce it [6,7,31,73]. Moreover, data from female ERα knockout mice show that aggressive behaviors are reduced under some circumstances and enhanced in others [57]. Neuroanatomical studies showed that the stimulation of the medial amygdala and the VMN increased aggression in rodents while lesions in these nuclei cause opposing effect [28,33,34,36]. Although both the medial amygdala and the VMN appear to modify aggressive behaviors, the role of estrogen receptors within these structures is unknown. Nevertheless, it can be proposed that estrogens within the VMN act to reduce aggressive behaviors. This would facilitate sexual interactions. Interestingly, both the display of lordosis and approach to a sexually active male depends on the ERα within the VMN [55,71], and both behaviors may require a reduced level of anxiety.

In the present series of experiments we determined how the absence of the ERα in the VMN or the MePDA affected social recognition, aggression and anxiety in ovariectomized female rats treated with estradiol + progesterone. To that end, a short hairpin RNA (shRNA) directed against the ERα gene coupled to a viral vector was infused into one of these structures. We decided to employ a sequential treatment with estrogen + progesterone in order to emulate the events occurring during the estrus cycle. Furthermore, estrogens induce the expression of progesterone receptors both in the medial amygdala [25,37] and the VMN, and this effect is basically mediated by the ERα [50]. Indeed, one of the most important cellular actions of estrogen is this induction of progesterone receptors. The omission of progesterone would, consequently, imply that one of the main actions of estrogens was ignored.

2. Materials and methods

2.1. Subjects

Male and female Wistar rats were obtained from Charles River WIGA (Sulzfeld, Germany). They were housed two per cage under a reversed light–dark cycle (12:12 h, lights off 1100). Food (RM1, Special Diets Services, Witham, Essex, England) and tap water were always available. Ambient temperature was maintained at 21 ± 1 °C and relative humidity was 55 ± 10%. Most females (250 g upon arrival to the animal facilities) were ovariectomized and some males (300 g upon arrival) were castrated under isoflurane anesthesia. The intact females were used for reproduction thereby assuring an adequate supply of juvenile rats for the social recognition test. Pups were weaned at 21 days and thereafter housed six per cage. For the behavioral tests, they were used between 23 and 26 days of age. All experimental procedures employed in the present experiment were approved by the National Animal Research Authority of Norway and were in agreement with the European Union council directive 86/609/EEC.

2.2. Stereotaxic surgery

About 2 weeks after ovariectomy some females received intracerebral infusions under ketamine/xylazine anesthesia (100 mg/kg and 10 mg/kg, respectively). After the females were fixed in a stereotaxic frame and small holes were drilled, a total of 2 μl of either an shRNA encoded within an AAV viral vector directed against the ERα gene (ERα shRNA) or with an shRNA containing a sequence direted against luciferase gene (AAV control) as well as an independent enhanced green fluorescent protein (EGFP) expression cassette to mark the injection site was infused. Bilateral cannulae (30 gauge) were aimed at either the VMN (coordinates were: anteroposterior, −2.80; mediolateral, ±.6; dorsoventral −9.6) or the mediodorsal posterior amygdala (MePDA; coordinates were: anteroposterior, −3.14; mediolateral ±3.6; dorsoventral, −8.2). Coordinates were based on the ([60]) atlas with the skull level. The infusion lasted 10 min and the cannulae were slowly withdrawn 5 min after the end of infusion.

2.3. Design of the shRNA employed for ERα silencing

An adeno-associated virus (AAV) vector was made to express a small hairpin RNA (shRNA) against either the sequence specific for the ERα gene (5′-GATCCCCGGCATGGAGCATCTCTACA CTTCCTGTCA TGTAGAGATGCTCCAT GCCTTTTTTGGAAT-3′ and 5′-CTAGATTCCAAAAAA GGCATGGAGCATCTCTACA TGACAGGAAG TGTAGAGATGCTCCATGCCGGG-3′) or the sequence specific for luciferase as control (5′-GATCCCCCCGCTGGAGAGCAACTGCAT CTTCCTGTCA ATGCAGTTGCTCTCCAGCGGTTTTTGGAA-3′ and 5′-CTAGTT-CCAAAAACCGCTGGAGAGCAACTGCAT TGACAGGAAG ATGCAGTTGCTCTCCA GCGGGGG-3′). The nucleotides specific for ERα or luciferase are underlined. The shRNA became incorporated into the neurons adjacent to the injection sites, and as soon as the shRNA was expressed, it blocked ERα gene expression for the rest of the animals' life. The shRNAs employed here have been described in detail elsewhere [55].

2.4. Design of experiment

Four groups of 13 rats each were used. (1) ERα shRNA infused into the VMN. (2) AAV control infused into the VMN. (3) ERα shRNA infused into the MePDA. (4) AAV control infused into the MePDA.

2.5. Behavioral testing

Three to four weeks after intracerebral infusion, experimental females were given estradiol benzoate (18 μg/kg) about 52 h before the tests were begun. Progesterone (1 mg/rat) was injected 48 h after estradiol and 4 h before the beginning of tests. Both steroids were purchased from Sigma, St. Louis, MO, dissolved in peanut oil and injected sc in 1 ml/kg and .2 ml/rat, respectively. These doses are known to produce a lordosis quotient close to 100 [2,69]. An equal number of experimental and control females were used simultaneously in each test. The VMN and MePDA groups were tested on different days.

2.5.1. Social recognition test

The females were housed in individual cages 1 h before the test. Shortly before the experimental session they were transferred to another room. A juvenile (23–26 days old) rat was put into a cylindrical plastic container (9 cm diameter, 11 cm high with open top) with air holes in the lid. Fifteen seconds before each exposure the lid was removed, and the container was then introduced into a female's cage in a horizontal position and left for 5 min. The juvenile invariably left the container, and all interactions with the experimental subject occurred consequently outside of the container. Fifteen min after removal the same juvenile was reintroduced into the female's cage in a clean container for another 5 min observation period. This was repeated until the female had been exposed to the juvenile 4 times. At the 5th exposure, a new juvenile was introduced and left for 5 min. The juvenile was placed into a clean container 5 min before being introduced into the female's cage. The same cylinder was used for all exposures, but it was thoroughly washed with unscented soap and then dried with paper towels between each exposure. Thus, there was no accumulation of odors in the container during the experiment. An incandescent light bulb provided a white light with an intensity of about 5 lux at the bottom of the cage. The females were left undisturbed in the room during the test without any observer present, and their behavior was videotaped for subsequent analysis.

The following behaviors were recorded: juvenile investigation (active sniffing and grooming of different parts of the juvenile), juvenile odor investigation (active sniffing of the container), container investigation (sniffing the outside of the container), sniffing other objects anywhere in the cage (exploration of the test cage), rearing, aggressive behaviors (the sum of kicking and biting the juvenile) and other active (locomotion, self-grooming, digging in bedding) as well as nonactive behaviors (sitting, lying down, both coded under the term of immobility) and freezing. The frequency and duration of these behaviors were determined from the videotapes with the help of the Observer XT software (Nodlus, Wageningen, the Netherlands).

2.5.2. Light/dark choice test

The test lasted 600 s and was performed in a two-compartment box consisting of one light chamber (20 cm × 30 cm × 45 cm), which was illuminated from the top with a white light producing an intensity of 600 lux at floor level, and one dark chamber (20 cm × 30 cm × 45 cm) with a light intensity of 5 lux at floor level. The chambers were separated by a black partition with a small opening (6 cm × 6 cm) at the bottom. Immediately after the test for social recognition, the animals were brought to an adjacent testing room and left undisturbed in their cage for 30 min. They were then introduced into the center of the dark chamber of the light/dark test apparatus, facing the light chamber.

A videotrack system (Ethovision Pro, Noldus, Wageningen, the Netherlands) determined the time the experimental subject spent in each chamber, the number of visits to each chamber, the latency to enter the dark chamber, and the latency to exit from the dark chamber (time after the first entry into the dark chamber until the first exit). The distance moved during the test, the mean velocity while moving, and the time of immobility were determined for both dark and light chambers and data are presented as total for the entire box.

2.5.3. Resident–intruder test

After the light/dark choice test, the animals were returned to the home cage for a 60 min rest. Then, a castrated male was introduced into the cage and left there for 10 min. The light intensity was about 5 lux. The rats were left undisturbed in the room, and were videotaped for subsequent analysis. The frequency and duration of the following behaviors were determined from the videotapes with the help of the Observer XT software (Nodlus, Wageningen, the Netherlands): Chasing; tail writhe (sinuous movement of the tail or part of the tail, with or without banging on the floor), piloerection, nose-off (the subject and the intruder stand immobile, facing each other); open mouth tooth display (open mouth displaying the incisors); sidling (one rat approaches the other sideways); belly groom; pushing; kicking; boxing; biting; wrestling; exploration (horizontal and vertical activity); digging; self-grooming.

2.6. Immunocytochemistry

The subjects were euthanized with carbon dioxide the day following the behavioral tests and immediately perfused with PBS followed by 4% paraformaldehyde (PFA). The brain was removed and postfixated overnight at 4 °C in 4% PFA. It was then rinsed with PBS and cryoprotected in PB containing 30% sucrose for 24 h at 4 °C. Then, the brains were frozen in isopentane cooled on dry ice, and transferred to a −80 °C freezer.

Brains were frozen-sectioned at 50 μm and the VMN or the MePDA sections were collected as appropriate. Sections were treated by antibodies against the ERα (polyclonal, 1:25,000; Upstate, Lake Placid, NY) and EGFP (GFP, Abcam, Cambridge, MA) in combination with secondary antibodies (biotinylated rabbit) and avidin–biotin peroxidase complex (ABC elite kit from Jackson Immunoresearch, West Grove, PA) to identify cells containing ERα and injection localization, respectively. After antibody reactions and several washings in PBS, sections were stained with diaminobenzidine (DAB). DAB revealed injection localization by brown coloration of EGFP while the ERα was colored in purple by the addition of nickel.

The number of ERα stained cells in the VMN and the MePDA was counted. Slices with anteroposterior coordinates from −3.10 to −3.20 for the MePDA and those with anteroposterior coordinates from −2.70 to −2.90 for the VMN were stained according to atlas coordinates [60]. Only those with the greatest ERα staining have been chosen. Photographs of each nucleus were taken by a combination of microscope (Nikon Eclipse E400) and camera (Nikon CoolPix 990). Then, pictures were transferred to a computer and opened by Photoshop software. Based on atlas coordinates with the skull level [60] a virtual pen was used to delineate the VMN and the MePDA. The number of stained cells was counted and divided by the surface of each nucleus in order to obtain a density (number of ERα/mm^2).

2.7. Data analysis

Only rats with bilateral brown coloration of EGFP in the MePDA or the VMN were included in the analysis. This coloration indicated successful bilateral virus infusions. For the social recognition test, rats killing the juvenile were excluded from analysis. This applied to 1 animal in the ERα shRNA VMN and to 2 animals in the AAV control VMN group.

A *t* test was used to evaluate the number of ERα immunoreactive cells in the groups treated with ERα shRNA and AAV control in the MePDA or the VMN.

Behavioral data from the two groups infused with ERα shRNA and AAV control into the MePDA were analyzed separately from the groups infused with ERα shRNA and AAV control into the VMN.

Social recognition data were analyzed with two-factor ANOVA for repeated measures on one factor. The between-groups factor was treatment (ERα shRNA and AAV control) while the within-groups factor was exposure (1–5). In case of nonhomogenous error variances, as determined by Levene's test, data were subjected to a logarithmic transformation. After a significant interaction, tests for simple effects within treatments as well as within exposures were performed. Following significant ANOVA, Tukey's HSD test was employed for determining differences between exposures. Data from the light/dark choice test and the resident–intruder tests were analyzed with *t* tests.

A one-tailed significance level of .05 was used to compare the first exposure to the others in the social interaction test. The use of a one-tailed significance level was justified by the fact that exploration of the juvenile always is reduced upon repeated exposition in intact rats. A two-tailed significance level of .05 was used for all other tests.

3. Results

3.1. Histology

Four rats in the group infused with ERα shRNA into the VMN had infusion sites outside of the intended nucleus. Consequently, there remained eight females in this group.

The number of ERα in the MePDA was significantly reduced in the animals infused with ERα shRNA compared to those infused with AAV control, $t(24) = 9.47$, $p < .001$ (Fig. 1A and C). In the same way, a significant reduction of ERα staining was observed in the animals infused with ERα shRNA into the VMN compared to animals infused with AAV control, $t(17) = 8.51$, $p < .001$ (Fig. 1A). Indeed, there was a reduction of ERα expression of about 81% in both structures. The suppression of ERα is site specific since the group infused with ERα shRNA or AAV control into the MePDA did not show significant difference in ERα staining in the medial posteroventral amygdala, $t(24) = 1.87$, *ns*. Likewise, the number of ERα in the arcuate nucleus was not significantly changed by infusion of ERα shRNA or AAV control into the VMN, $t(17) = .52$, *ns* (Fig. 1B).

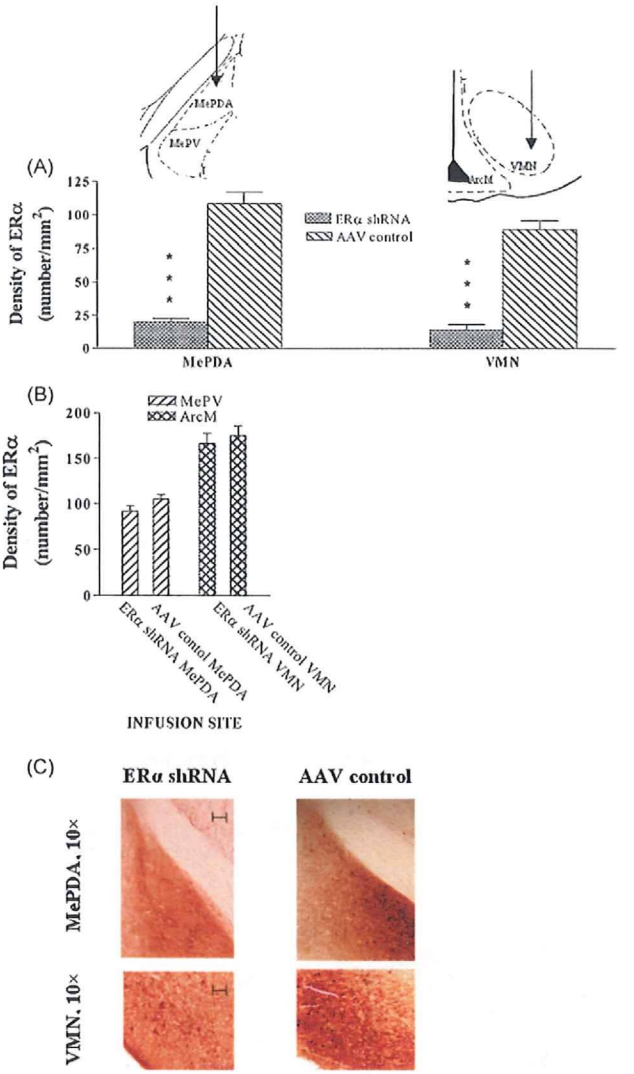

Fig. 1. (A) Mean ± SEM number of ERα in the MePDA and VMN after bilateral infusion of an AAV-associated shRNA directed against the ERα gene (abbreviated ERα snRNA in the figure; MePDA, $n = 13$; VMN, $n = 8$) or a control shRNA (abbreviated AAV control in the figure; MePDA, $n = 13$; VMN, $n = 11$) into these structures. The sites of injections are illustrated above the bars (only one side is shown). (B) Number of ERα in structures adjacent to the infusion sites, the posteroventral amygdala (MePV) for the MePDA and the arcuate nucleus (ArcM) for the VMN. (C) Immunocytochemical staining of typical brain slices in the MePDA and in the VMN. Scale bar is 200 μm. Notice a reduction of ERα staining in the MePDA and in the VMN in animals infused with ERα shRNA compared to animals with AAVcontrol. ERα shRNA is the group of females injected by shRNA against ERα gene either in the MePDA or in the VMN; AAV control is the group of females injected by inactive shRNA either in the MePDA or in the VMN. ***, $p < .001$ compared to ERα shRNA.

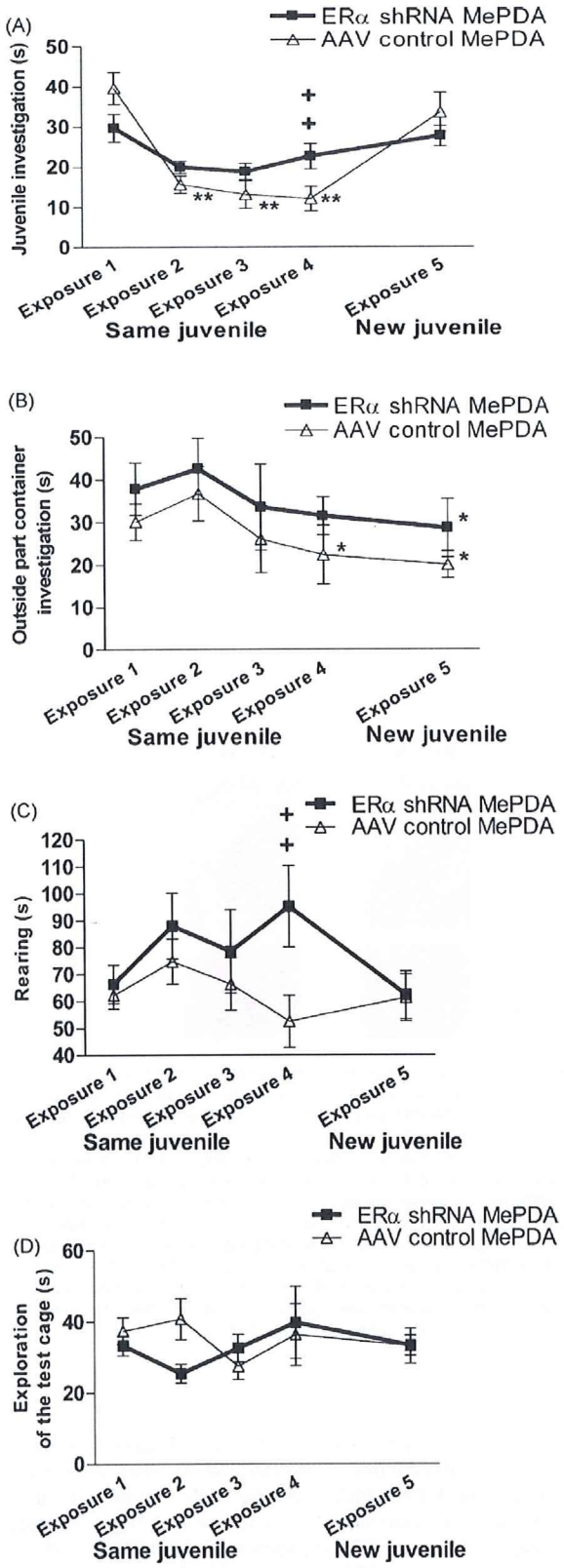

Fig. 2. Mean ± SEM of parameters of behaviors in the social recognition test. (A) time (in s) spent in juvenile investigation; (B) time (in s) spent in outside part of the container (with juvenile inside) investigation; (C) time (in s) spent in rearing and (D) time (in s) spent in exploration of the test cage in female rats with a reduced number of ERα in the MePDA and the corresponding controls. For further details, see legend

3.2. Behavioral effects of ERα knockdown

3.2.1. Social recognition

There was no effect of exposure or treatment and no interaction between exposure and treatment with regard to locomotion (all *ps* > .09). Hence, this parameter is not further mentioned.

As illustrated in Fig. 2A, social recognition was affected in the subjects with reduced ERα expression in the MePDA. There was a significant main effect of exposure on juvenile investigation, $F(4,96) = 19.99$, $p < .001$, and a significant interaction treatment x exposure, $F(8, 96) = 3.95$, $p < .01$. There was no main effect of treatment, $F(1, 24) = .61$, *ns*. Tests of simple effects of exposure within treatment showed that the females infused with ERα shRNA into the MePDA spent about the same time investigating the juvenile at each exposure, $F(4, 96) = 2.90$, *ns*, even at the 5th exposure, where the familiar juvenile was replaced by a new one. In contrast, animals infused with AAV control into the MePDA spent less time investigating the juvenile during the second, third and forth presentation compared to the first, $F(4, 96) = 21.04$, $p < .001$. When a new juvenile was introduced at the fifth exposure, the time the females spent investigating the juvenile was similar to that spent at the first presentation. Thus, the control group demonstrated no impairment of social recognition. The analysis of the effect of treatment within each exposure showed that the group infused with ERα shRNA into the MePDA investigated the familiar juvenile longer than the group infused with AAV control into the MePDA at the 4th exposure. No group differences were found at the other exposures.

There was a significant effect of exposure on the time spent investigating the container, $F(4, 96) = 9.33$, $p < .001$ but there was no interaction treatment x exposure, $F(8, 96) = .08$, *ns*, and no main effect of treatment, $F(1, 24) = 1.23$, *ns*. Thus, the reduction in investigation of an inanimate object associated with repeated exposures was not affected in the subjects with ERα knockdown in the MePDA. Data are illustrated in Fig. 2B.

Regarding rearing there was a significant interaction treatment × exposure, $F(8, 96) = 2.53$, $p < .05$ but no main effect of exposure, $F(4, 96) = 2.28$, *ns*, or treatment, $F(1, 24) = 1.58$, *ns*. Tests of simple effects of treatment within exposure showed that the subjects infused with ERα shRNA into the MePDA spent more time rearing than the animals infused with AAV control at Exposure 4, $F(1, 24) = 5.65$, $p < .05$. Data are summarized in Fig. 2C.

Concerning exploration of the test cage, no significant effect was found for exposure, $F(4, 96) = .60$, *ns*, or treatment, $F(1, 24) = .35$, *ns*. The interaction treatment × exposure was also nonsignificant, $F(8, 96) = 1.13$, *ns*. Data are shown in Fig. 2D.

Social recognition was not affected in the subjects infused with ERα shRNA into the VMN. There was a significant effect of exposure on juvenile investigation, $F(4, 68) = 20.02$, $p < .001$ while there was no interaction treatment × exposure, $F(8, 68) = .91$, *ns*, and no effect of treatment, $F(1, 17) = 1.65$, *ns*. Data are summarized in Fig. 3A.

There was a significant effect of exposure on the time spent investigating the outside of the container, $F(4, 68) = 3.17$, $p < .001$ but there was no interaction treatment × exposure, $F(8, 68) = .31$, *ns*, and no effect of treatment, $F(1, 17) = .85$, *ns*. Data are illustrated in Fig. 3B.

Concerning rearing, there was no significant interaction treatment × exposure, $F(8, 68) = .42$, *ns*, no main effect of exposure, $F(4, 68) = 1.90$, *ns*, or of treatment, $F(1, 17) = .97$, *ns*. Data are summarized in Fig. 3C.

to Fig. 1. *, represent a significant decrease between each session as compared to the first session, $p < .05$; **, $p < .01$. Lines indicate significant differences between groups: ++, $p < .01$.

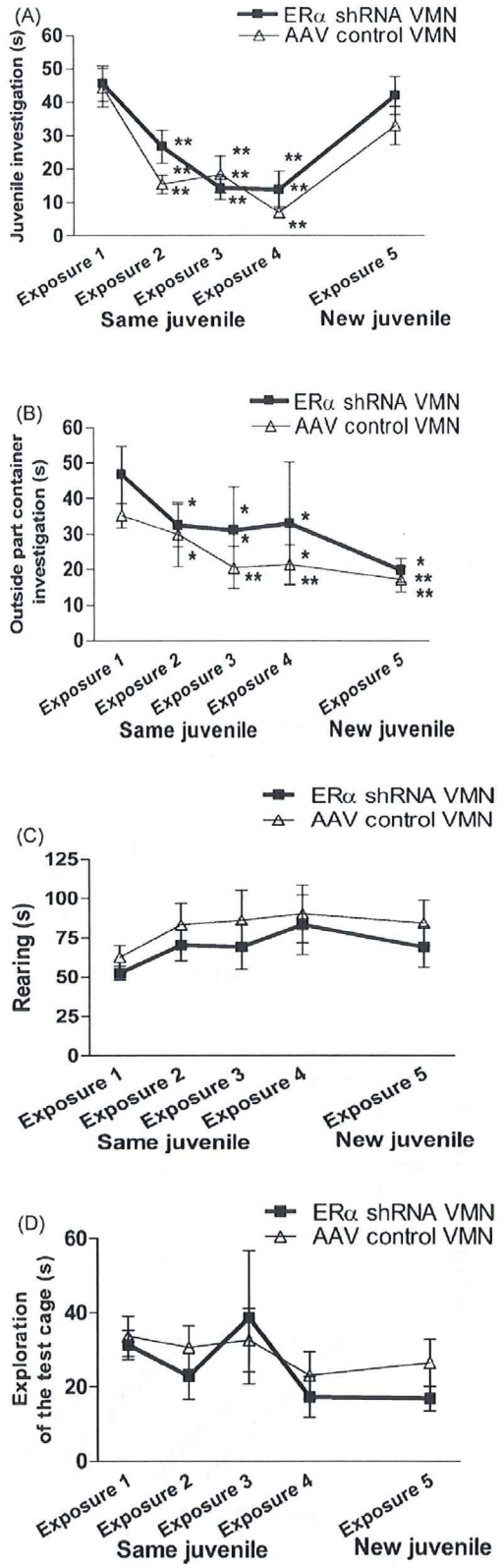

Fig. 3. Mean ± SEM of parameters of behaviors in the social recognition test. (A) time (in s) spent in juvenile investigation; (B) time (in s) spent in outside part of the container (with juvenile inside) investigation; (C) time (in s) spent in rearing and (D) time (in s) spent in exploration of the test cage in female rats with a reduced number of ERα in the VMN and the corresponding controls. For further details, see legend to Fig. 1. *, represent a significant decrease between each session as compared to the first session, $p < .05$; **, $p < .01$. Lines indicate significant differences between groups: ++, $p < .01$.

There was no main effect of exposure on exploration of the test cage, $F(4, 68) = 1.9$, *ns*, and there was no effect of treatment, $F(1, 17) = .97$, *ns*, and no interaction treatment × exposure, $F(8, 68) = .42$, *ns*. Data are shown in Fig. 3D.

3.2.1.1. Aggression, self-grooming and freezing during social recognition test. In the groups infused with ERα shRNA and AAV control into the MePDA, there was no effect of exposure or treatment and no interaction between exposure and treatment with regard to aggression, self-grooming and freezing (all *ps* > .10; data not shown). Interestingly, the frequency of aggressive behaviors in these groups was close to 0. Hence, this parameter is not further mentioned in the MePDA groups.

Like the groups treated in the MePDA, subjects infused with the AAV control in the VMN displayed almost no aggressive behaviors. However, the group infused with ERα shRNA into the VMN displayed an increased higher frequency of these behaviors. ANOVA comparing this group to the one infused with AAV control into the VMN showed that there was a significant main effect of exposure, $F(4, 68) = 6.10$, $p < .001$, and treatment, $F(1, 17) = 7.50$, $p < .05$ as well as a significant interaction treatment × exposure, $F(8, 68) = 2.40$, $p < .05$. Tests for simple effects of treatment within each exposure showed that aggression was enhanced at the first two presentations of the juvenile (Exposures 1 and 2) $F(1, 17) = 4.53$, $p < .05$, and $F(1, 17) = 4.20$, $p < .05$, respectively, and at presentation of the new juvenile (Exposure 5), $F(1, 17) = 7.87$, $p < .05$. Data are illustrated in Fig. 4A.

Concerning grooming, there was a significant main effect of exposure, $F(4, 68) = 3.39$, $p < .01$, and a significant interaction treatment × exposure, $F(8, 68) = 3.75$, $p < .01$. There was no main effect of treatment, $F(1, 17) = 2.14$, *ns*. Tests of simple effect of exposure within treatment revealed that the subjects infused with ERα shRNA into the VMN spent more time grooming at the last two presentations of the familiar juvenile (Exposures 3 and 4) than they did at the first presentation (Exposure 1), $F(4, 68) = 5.83$, $p < .001$. Moreover, Tukey's HSD test demonstrated that the ERα shRNA VMN group spent more time grooming at the third and the fourth presentation of the juvenile (Exposures 3 and 4) than its control group, $F(1, 17) = 4.52$, $p < .05$, and $F(1, 17) = 5.12$, $p < .05$, respectively. Thus, grooming showed a pattern that was the inverse of pattern that which was observed with regard to aggression in the ERα shRNA VMN group. Data are summarized in Fig. 4B.

Regarding freezing, there was a significant main effect of exposure, $F(4, 68) = 3.39$, $p < .05$, and a significant interaction treatment × exposure, $F(8, 68) = 3.50$, $p < .01$. There was no main effect of treatment, $F(1, 17) = 1.86$, *ns*. Tests of simple effect of exposure within treatment revealed that the subjects infused with ERα shRNA into the VMN spent more time freezing at the last two presentations of the familiar juvenile (Exposures 3 and 4), and at presentation of the new juvenile (Exposure 5) than they did at the first presentation (Exposure 1), $F(4, 68) = 10.59$, $p < .01$. Likewise, Tukey's HSD test demonstrated that freezing was enhanced at the last presentation of the familiar juvenile (Exposure 4) in the subjects infused with ERα shRNA into the VMN compared to those infused with AAV control into the VMN, $F(1, 17) = 7.16$, $p < .01$. Data are shown in Fig. 4C.

3.2.2. Light/dark choice test

The subjects with reduced number of ERα in the MePDA showed an increase in the time spent in as well as the number of visit to the light chamber, $t(24) = 2.49$, $p < .05$, and $t(24) = 2.95$, $p < .01$, respectively. Data are summarized in Fig. 5A and B. Likewise, this group moved a longer distance than the control, $t(24) = 2.60$, $p < .05$. Data are illustrated in Fig. 5C.

The time spent in the light chamber or the ambulatory activity was not affected in the group infused with ERα shRNA into the VMN

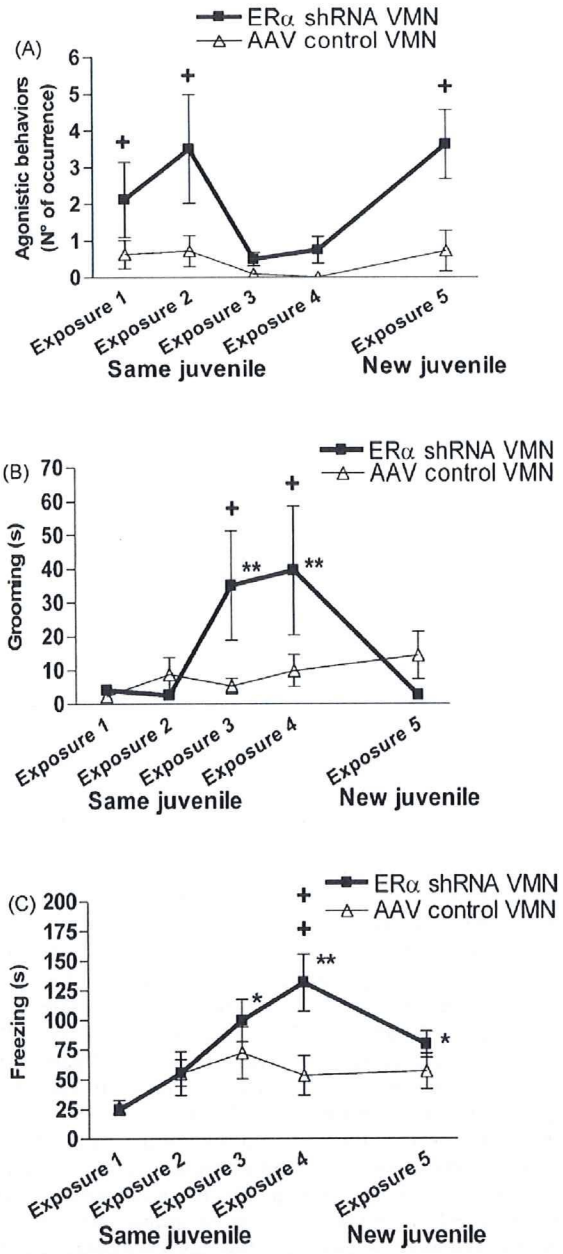

Fig. 4. Mean ± SEM of parameters of behaviors in the social recognition test. (A) number of aggressive behaviors bouts against juvenile; (B) time (in s) spent in grooming and (C) time (in s) spent in freezing in female rats with a reduced number of ERα in the VMN and the corresponding controls. For further details, see legend to Fig. 1. *, represent a significant decrease between each session as compared to the first session, $p < .05$; **, $p < .01$. Lines indicate significant differences between groups: ++, $p < .01$.

(all comparisons between the VMN groups had $ps > .90$). Data are shown in Fig. 5A–C.

3.2.3. *Resident–intruder test*

Aggressive behaviors were not affected in the group infused with ERα shRNA either into the VMN or into the MePDA. Indeed, the *t* test revealed that the number of aggressive behaviors in the subjects infused with ERα shRNA into the VMN was not significantly different from the number of aggressive behaviors displayed by the subjects infused with AAV control into the VMN, $t(17) = .487$, *ns*. Likewise, the *t* test showed that the number of aggressive behav-

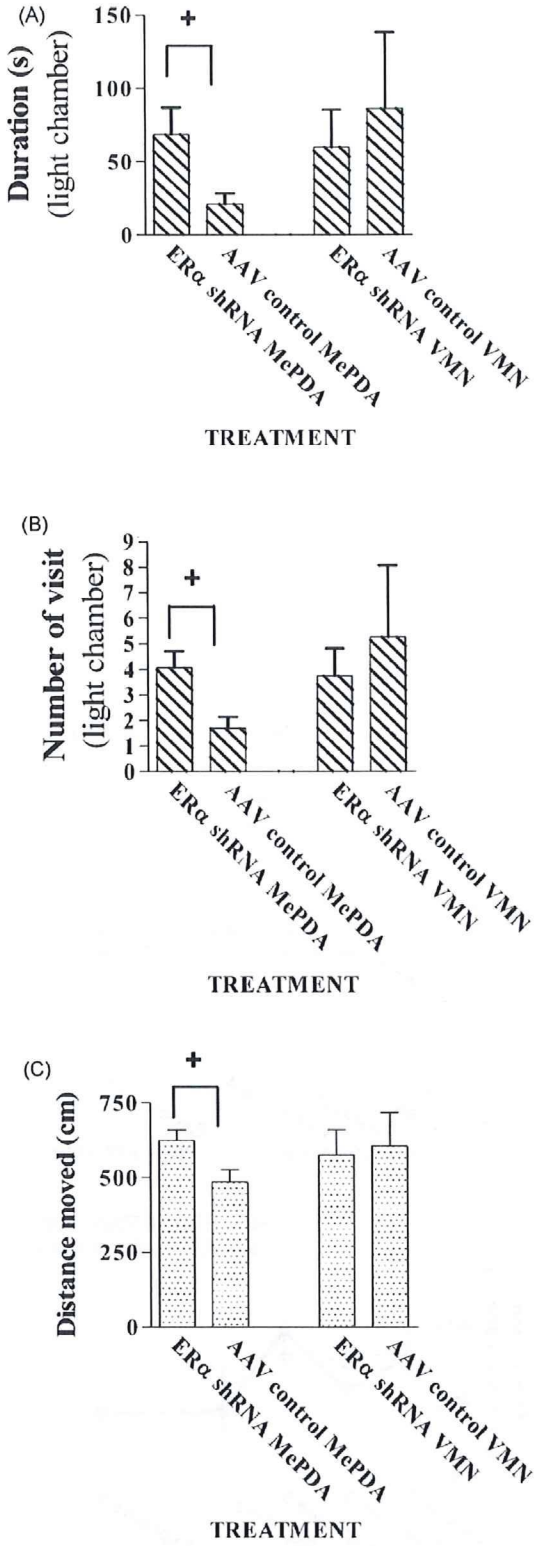

Fig. 5. (A) time (in s) spent; (B) number of visit in the light chamber and (C) distance moved (in cm) in the light and dark chambers by female rats with a reduced number of ERα in the MePDA or the VMN and the corresponding controls. For further details, see legend to Fig. 1. Data are mean ± SEM. Lines indicate significant differences between groups: +, $p < .05$.

Table 1
Mean ± SEM aggressive behaviors in the resident–intruder test in female rats with a reduced number of ERα in the MePDA or the VMN and the corresponding controls.

Groups	Aggressive behaviors
ERα shRNA VMN	2.7 ± 1.2
AAV control VMN	4.5 ± 2.9
ERα shRNA MePDA	2.4 ± 1.4
AAV control MePDA	3.5 ± 1.7

iors in the group infused with ERα shRNA into the MePDA was similar to the group infused with AAV control into this structure, $t(24) = .472$, *ns*. No significant difference was found when the number of kickings and bitings was analyzed separately (all *ps* > .21). Moreover, no difference was found in other social and exploratory activities, or anxiety-related behaviors. Data are shown in Table 1.

4. Discussion

4.1. Efficiency and specificity of ERα knockdown

The shRNA used in this experiment produced a substantial reduction of ERα expression in the VMN and the MePDA. At the same time the number of receptors was unaffected in structures adjacent to the target sites, thereby demonstrating the efficiency and specificity of the shRNA. The shRNA employed here does not modify ERβ expression [55], making it reasonable to propose that the reduction of ERα expression in the VMN and the MePDA accounts for all behavioral effects observed in the present experiments. Nevertheless, it is not possible to exclude that the few remaining ERα had some effect. The effects reported here might be amplified by a total suppression of this receptor.

4.2. Effects of ERα knockdown on social recognition

A specific reduction of the ERα in the MePDA suppressed social recognition in female rats. Indeed, such females showed no reduced response to repeated presentation of a conspecific juvenile and no increased response when the familiar juvenile was replaced with a new one. In contrast, the control group demonstrated habituation and dishabituation of juvenile exploration. Moreover, females with few ERα in the MePDA showed a reduced exploration of the exterior of the container upon repeated exposure. In fact, they were not different from the control group. This suggests that the deficient habituation to the juvenile was not due to a generalized lack of object recognition, but to a specific failure to habituate to a social object. It is worth noting that the decreased exploration of the non-social object was of less magnitude than the decrease of investigation of the juvenile. This observation could be explained by the fact that the direct social interaction between the female and the juvenile has a baseline level far above that of the exterior part of the container.

In order to display the habituation/dishabituation response underlying the paradigm employed here the experimental subject needs to recognize the juvenile used at the repeated exposures, and distinguish the new juvenile from the previous one. Present data show that the ERα within the MePDA is necessary for this. To the contrary, the ERα in the VMN does not appear to contribute to social recognition. Present data also reinforce the notion that recognition of social and non-social objects depend on different processes as suggested earlier [11].

Knockdown of ERα in the MePDA did not modify horizontal exploration. Hence, the absence of habituation to the juvenile in these females cannot be explained by a general alteration of exploratory activities. Furthermore, it is doubtful whether exploratory activities interfere with juvenile exploration, since females with few ERα in the MePDA displayed more vertical activity than controls at the last presentation of the familiar juvenile, yet they spent more time exploring it than controls.

Social recognition in rodents has been shown to be based on olfaction [17,66], although auditory and visual signals may contribute under some circumstances [62]. The main and accessory olfactory systems project to the anterior and posterior cortical nuclei of the amygdala, respectively. The accessory olfactory system also projects to the anteromedial nuclei of the amygdala [68]. The MePDA is then reached by intrinsic connections [12,41]. Indeed, activation of the olfactory bulbs as well as the medial and cortical amygdala was demonstrated in female rats after an encounter with a conspecific pup [22] and in mice exposed to a juvenile [65].

It is conceivable that the ERα in the MePDA somehow modulates olfactory input. However, studies in aromatase knockout mice have shown an intact fos response to sexually relevant olfactory cues [8]. Likewise, adult ovariectomized mice show the same fos response to male odors regardless of whether they are treated with estradiol or not [27]. These data suggest that estrogens are not important for olfactory processing. Alternatively, activity at the ERα receptor may facilitate memory. Social recognition does not only depend on the capacity to distinguish one individual from another, but also on the capacity to remember the individual characteristics from one exposure to the next. While long-term treatments with estradiol have been repeatedly reported to improve some kinds of memory [16,44], there were no changes in performance on a memory task during the estrous cycle [10] suggesting that short-term variations in estrogen availability are not likely to have functionally relevant effects on memory. Although there is one study reporting short-latency effects of estradiol on memory, the involvement of ERs is doubtful since 17α- and 17β-estradiol were equally effective [43]. The intact habituation/dishabituation response to the cylinder observed even in the shRNA group reinforces the idea that ERα effects on memory are not involved. It is, indeed, possible that the effect of ERα silencing in the MePDA is specific for the recognition of a social stimulus.

4.3. Effects of ERα knockdown in the VMN on aggression toward the juvenile and anxiety-related behaviors

From the MePDA, the olfactory information reaches the preoptic area and the VMN mainly through the bed nucleus of the stria terminalis [12]. ERα knockdown in the VMN enhanced aggression towards a conspecific juvenile at the first two exposures. The ERα shRNA females showed also enhanced aggression when the novel juvenile was introduced. Since females with ERα knockdown in the VMN showed normal social recognition, we can reasonably infer that the juvenile became familiar after several exposures and did not, therefore, elicit aggression from the female. At exposures 3 and 4 the ERα shRNA females showed a high level of grooming and freezing. Since enhanced grooming and freezing is thought to be a response to anxiogenic stimuli [72], this observation may suggest that the juvenile had lost its capacity to evoke aggressive responses and instead produced anxiety.

4.4. Effects of ERα knockdown in the light/dark choice test

The silencing of ERα in the MePDA reduced anxiety. The females with few ERα in the MePDA spent more time in the light chamber and entered it more often than control females. They also presented an augmentation of distance moved in the entire device (light and dark chambers) compared to controls. Thus, females with intact ERα in the MePDA showed more anxiety-like behavior than females with few ERα. This fact suggests that stimulation of the ERα in the MePDA has an anxiogenic effect. This could explain why females with ERα knockdown in the MePDA showed more vertical activ-

ity than controls at the last presentation of the familiar juvenile during the social recognition test. Although rearing is not strictly determined by anxiety, it is more frequent when the level of anxiety is low [25,40]. The absence of a group difference with regard to horizontal activity may be explained by the fact that this kind of activity is less sensitive to variations in anxiety.

The activity of estrogens-treated female rats has been shown to increase in safe environments [9,76] while it is reduced in threatening contexts [18]. It has been proposed that these opposing behavioral effects are consequences of estrogens' role in increasing arousal [61]. Heightened arousal increases locomotor activity in safe environments while it produces an anxiety response in threatening environments. Present results reinforce this idea because females with reduced anxiety also showed enhanced locomotor activity. The mechanisms by which estrogens act on anxiety in the MePDA remain unknown.

4.5. The possible role of progesterone receptors

It could be argued that some or all of the effects reported here are not directly dependent on the ERα but on a reduced availability of progesterone receptors in animals with ERα knockdown. Consequently, what has actually been observed here are the consequences of deficient progesterone receptor activation in the VMN or the MePDA. In the case of anxiety-like behaviors, this is unlikely, though, since estradiol, progesterone and estradiol + progesterone have similar effects in several tests of anxiety (e.g. [42]). This suggests that progesterone actions on non-estrogen inducible progesterone receptors are important, and these receptors should be unaffected in the animals used in the present experiment. With regard to aggression it is difficult to attribute a specific function to progesterone in view of the fact that both reduction and increase have been reported after progesterone treatment [4,5]. The role of progesterone in social recognition is essentially unknown. Nevertheless, it seems that alterations in progesterone receptors cannot be excluded as the ultimate explanation for some of the effects observed here. Since the reduction of progesterone receptor availability would be limited to estrogen inducible receptors, therefore a direct result of ERα knockdown, it is not unwarranted to maintain that the ERα also is involved in these behaviors. Present data do not allow for any evaluation of the specific role of progesterone receptors, but this was not the purpose of these experiments.

4.6. The possible role of ERβ

There are many examples of interactions between the ERα and the ERβ, both cooperative and opposing (e.g. [24,79]). It could be argued that some of the effects observed after reduction of the ERα are due to estrogen action at the ERβ. The ERβ-mediated effects may be obscured by an opposing action at the ERα in the intact animal. Although theoretically possible, opposing estrogen actions on the ERs would make little physiological sense. In the intact animal, both receptors would be activated simultaneously and the net effect would be nil. Even though some experimental manipulations may reveal opposing actions, their importance should not be exaggerated. In the particular case of social interaction, there is actually evidence against opposing actions of the ERs [13,15,70].

4.7. The indirect role of ERα in the MePDA and the VMN for reproduction

The ERα in the VMN has been reported to be necessary for the display of receptivity and proceptivity as well as for sexual incentive motivation while knockdown of this receptor in the MePDA does not affect any of these behaviors [71]. However, the ERα in the MePDA is necessary for social recognition. It is well known that sexually receptive female rats are capable to recognize their sexual partners [21], and this recognition may have consequences for their sexual behavior. For example, a sexually exhausted female will reinitiate copulation with a novel male [1]. More subtle effects of mate recognition are likely to exist and to be important for reproductive efficiency. We suggest that estrogens assure appropriate sexual behavior through actions on the ERα within the VMN while this receptor in the MePDA participates in other functions, indirectly important for reproduction, like social, including mate, recognition.

In addition to the assurance of appropriate sexual behavior, the ERα in the VMN modulates the response to a threatening situation and some kinds of aggression. It is noteworthy that no effect of ERα knockdown was found in the resident–intruder test. The intruder, a castrated male, should not provoke a reaction much different from that produced by the juvenile. However, while the castrated male was introduced into the female's home cage, a safe environment, the juvenile was introduced into an observation cage where the female had been placed shortly before the test, in an unknown room. It is most likely that this is a threatening situation. Another interesting finding is that the silencing of ERα in the VMN had no effect in the light/dark choice test. Thus, the anxious reaction to a threatening environment seems to be limited to a social context. This could be another manifestation of the different effects of estrogens in different contexts. It appears to be most adaptive to display fear and aggression rather than sexuality in threatening contexts, but to be active and sociable in safe contexts. Present results together with earlier observations suggest that the combined actions of the ERα in the VMN and MePDA assure that this will be the case.

In conclusion, present data do not allow for any definite conclusion as to the exact mechanisms by which ERα knockdown modifies social recognition, aggression and anxiety. Nevertheless, it is hoped that present results contribute to an understanding of the quite intricate effects of estrogens, particularly within the VMN, underlying the behavioral modifications necessary for successful reproductive behavior in the female rat.

Acknowledgements

Expert technical assistance was provided by Ragnhild Osnes, Stig Rune Olsen, Carina Sørensen and Nina Løvhaug. Financial support was received from the University of Tromsø (to TS and AÅ) and from grants MH 38273 and HD 05751 to D.W. Pfaff.

References

[1] Ågmo A, Ellingsen E, Turi AL, Larsson K. A female Coolidge effect. In: Paper presented at the annual meeting of the International Behavioral Neuroscience Society, Capri. 2002.
[2] Ågmo A, Turi AL, Ellingsen E, Kaspersen H. Preclinical models of sexual desire: conceptual and behavioral analyses. Pharmacol Biochem Behav 2004;78:379–404.
[3] Adamec RE, Morgan HD. The effect of kindling of different nuclei in the left and right amygdala on anxiety in the rat. Physiol Behav 1994;55:1–12.
[4] Albert DJ, Jonik RH, Walsh ML. Hormone-dependent aggression in male and female rats: experiential, hormonal, and neural foundations. Neurosci Biobehav Rev 1992;16:177–92.
[5] Albert DJ, Jonik RH, Walsh ML. Interaction of estradiol, testosterone, and progesterone in the modulation of hormone-dependent aggression in the female rat. Physiol Behav 1992;52:773–9.
[6] Albert DJ, Petrovic DM, Walsh ML. Ovariectomy attenuates aggression by female rats cohabiting with sexually active sterile males. Physiol Behav 1989;45:225–8.
[7] Albert DJ, Walsh ML, Gorzalka BB, Siemens Y, Louie H. Testosterone removal in rats results in a decrease in social aggression and a loss of social-dominance. Physiol Behav 1986;36:401–7.
[8] Aste N, Honda S, Harada N. Forebrain Fos responses to reproductively related chemosensory cues in aromatase knockout mice. Brain Res Bull 2003;60:191–200.

[9] Beatty WW. Gonadal hormones and sex differences in nonreproductive behaviors. In: Gerall AA, Moltz H, Ward IL, editors. Sexual differentiation. New York: Plenum Press; 1992. p. 85–128.
[10] Berry B, McMahan R, Gallagher M. Spatial learning and memory at defined points of the estrous cycle: effects on performance of a hippocampal-dependent task. Behav Neurosci 1997;111:267–74.
[11] Bielsky IF, Young LJ. Oxytocin, vasopressin, and social recognition in mammals. Peptides 2004;25:1565–74.
[12] Canteras NS, Simerly RB, Swanson LW. Connections of the posterior nucleus of the amygdala. J Comp Neurol 1992;324:143–79.
[13] Choleris E, Gustafsson JA, Korach KS, Muglia LJ, Pfaff DW, Ogawa S. An estrogen-dependent four-gene micronet regulating social recognition: a study with oxytocin and estrogen receptor-alpha and -beta knockout mice. Proc Nat Acad Sci USA 2003;100:6192–7.
[14] Choleris E, Little SR, Mong JA, Puram SV, Langer R, Pfaff DW. Microparticle-based delivery of oxytocin receptor antisense DNA in the medial amygdala blocks social recognition in female mice. Proc Nat Acad Sci USA 2007;104:4670–5.
[15] Choleris E, Ogawa S, Kavaliers M, Gustafsson JA, Korach KS, Muglia LJ, et al. Involvement of estrogen receptor alpha, beta and oxytocin in social discrimination: a detailed behavioral analysis with knockout female mice. Genes Brain Behav 2006;5:528–39.
[16] Daniel JM, Fader AJ, Spencer AL, Dohanich GP. Estrogen enhances performance of female rats during acquisition of a radial arm maze. Horm Behav 1997;32:217–25.
[17] Dantzer R, Tazi A, Bluthe RM. Cerebral lateralization of olfactory mediated affective processes in rats. Behav Brain Res 1990;40:53–60.
[18] DiazVeliz G, Soto V, Dussaubat N, Mora S. Influence of the estrous-cycle, ovariectomy and estradiol replacement upon the acquisition of conditioned avoidance responses in rats. Physiol Behav 1989;46:397–401.
[19] Ferguson JN, Aldag JM, Insel TR, Young LJ. Oxytocin in the medial amygdala is essential for social recognition in the mouse. J Neurosci 2001;21:8278–85.
[20] Fernandez-Guasti A, Martinez-Mota L, Estrada-Camarena E, Contreras CM, Lopez-Rubalcava C. Chronic treatment with desipramine induces an estrous cycle-dependent anxiolytic-like action in the burying behavior, but not in the elevated plus-maze test. Pharmacol Biochem Behav 1999;63:13–20.
[21] Ferreira-Nuño A, Morales-Otal A, Paredes RG, Velázquez-Moctezuma J. Sexual behavior of female rats in a multiple-partner preference test. Horm Behav 2005;47:290–6.
[22] Fleming AS, Suh EJ, Korsmit M, Rusak B. Activation of Fos-like immunoreactivity in the medial preoptic area and limbic structures by maternal and social interactions in rats. Behav Neurosci 1994;108:724–34.
[23] Frye CA, Walf AA. Estrogen and/or progesterone administered systemically or to the amygdala can have anxiety-reducing, fear-reducing, and pain-reducing effects in ovariectomized rats. Behav Neurosci 2004;118:306–13.
[24] Gonzales KL, Tetel MJ, Wagner CK. Estrogen receptor (ER) β modulates ER α responses to estrogens in the developing rat ventromedial nucleus of the hypothalamus. Endocrinology 2008;149:4615–21.
[25] Greco B, Allegretto EA, Tetel MJ, Blaustein JD. Coexpression of ER beta with ER alpha and progestin receptor proteins in the female rat forebrain: effects of estradiol treatment. Endocrinology 2001;142:5172–81.
[26] Grossman SP, Aggression. avoidance, and reaction to novel environments in female rats with ventromedial hypothalamic-lesions. J Comp Physiol Psychol 1972;78:274–83.
[27] Halem HA, Cherry JA, Baum MJ. Vomeronasal neuroepithelium and forebrain Fos responses to male pheromones in male and female mice. J Neurobiol 1999;39:249–63.
[28] Hansen S. Medial hypothalamic involvement in maternal aggression of rats. Behav Neurosci 1989;103:1035–46.
[29] Hiroi R, Neumaier JF. Differential effects of ovarian steroids on anxiety versus fear as measured by open field test and fear-potentiated startle. Behav Brain Res 2006;166:93–100.
[30] Hlinak Z. Social recognition in ovariectomized and estradiol-treated female rats. Horm Behav 1993;27:159–66.
[31] Ho HP, Olsson M, Westberg L, Melke J, Eriksson E. The serotonin reuptake inhibitor fluoxetine reduces sex steroid-related aggression in female rats: an animal model of premenstrual irritability? Neuropsychopharmacology 2001;24:502–10.
[32] Hughes ZA, Liu F, Platt BJ, Dwyer JM, Pulicicchio CM, Zhang GM, et al. WAY-200070, a selective agonist of estrogen receptor beta as a potential novel anxiolytic/antidepressant agent. Neuropharmacology 2008;54:1136–42.
[33] Kemble ED, Blanchard DC, Blanchard RJ, Takushi R. Taming in wild rats following medial amygdaloid-lesions. Physiol Behav 1984;32:131–4.
[34] Kemble ED, Davies VA. Effects of prior environmental enrichment and amygdaloid-lesions on consumatory behavior, activity, predation, and shuttlebox avoidance in male and female rats. Physiol Psychol 1981;9:340–6.
[35] Koss WA, Gehlert DR, Shekhar A. Different effects of subchronic doses of 17-beta estradiol in two ethologically based models of anxiety utilizing female rats. Horm Behav 2004;46:158–64.
[36] Kruk MR, Vanderlaan CE, Mos J, Vanderpoel AM, Meelis W, Olivier B. Comparison of aggressive-behavior induced by electrical-stimulation in the hypothalamus of male and female rats. Prog Brain Res 1984;61:303–14.
[37] Kudwa AE, Harada N, Honda SI, Rissman EF. Regulation of progestin receptors in medial amygdala: estradiol, phytoestrogens and sex. Physiol Behav 2009;97:146–50.
[38] Lee AW, Devidze N, Pfaff DW, Zhou J. Functional genomics of sex hormone-dependent neuroendocrine systems: specific and generalized actions in the CNS. Prog Brain Res 2006;158:243–72.
[39] Lee AW, Kyrozis A, Chevaleyre V, Kow LM, Zhou J, Devidze N, et al. Voltage-dependent calcium channels in ventromedial hypothalamic neurones of postnatal rats: modulation by oestradiol and phenylephrine. J Neuroendocrinol 2008;20:188–98.
[40] Lever C, Burton S, O'Keefe J. Rearing on hind legs, environmental novelty and, the hippocampal formation. Rev Neurosci 2006;17:111–33.
[41] Licht G, Meredith M. Convergence of main and accessory olfactory pathways onto single neurons in the hamster amygdala. Exp Brain Res 1987;69:7–18.
[42] Llaneza DC, Frye CA. Progestogens and estrogen influence impulsive burying and avoidant freezing behavior of naturally cycling and ovariectomized rats. Pharmacol Biochem Behav 2009;93:337–42.
[43] Luine VN, Jacome LF, MacLusky NJ. Rapid enhancement of visual and place memory by estrogens in rats. Endocrinology 2003;144:2836–44.
[44] Luine VN, Richards ST, Wu VY, Beck KD. Estradiol enhances learning and memory in a spatial memory task and effects levels of monoaminergic neurotransmitters. Horm Behav 1998;34:149–62.
[45] Lund TD, Rovis T, Chung WCJ, Handa RJ. Novel actions of estrogen receptor-beta on anxiety-related behaviors. Endocrinology 2005;146:797–807.
[46] Marcondes FK, Miguel KJ, Melo LL, Spadari-Bratfisch RC. Estrous cycle influences the response of female rats in the elevated plus-maze test. Physiol Behav 2001;74:435–40.
[47] Markham JA, Juraska JM. Social recognition memory: influence of age, sex, and ovarian hormonal status. Physiol Behav 2007;92:881–8.
[48] Mcewen BS, Alves SE. Estrogen actions in the central nervous system. Endocr Rev 1999;20:279–307.
[49] Milani H, Graeff FG. Gaba-benzodiazepine modulation of aversion in the medial hypothalamus of the rat. Pharmacol Biochem Behav 1987;28:21–7.
[50] Moffat CA, Rissman EF, Shupnik MA, Blaustein JD. Induction of progestin receptors by estradiol in the forebrain of estrogen receptor-alpha gene-disrupted mice. J Neurosci 1998;18:9556–63.
[51] Mora S, Dussaubat N, DiazVeliz G. Effects of the estrous cycle and ovarian hormones on behavioral indices of anxiety in female rats. Psychoneuroendocrinology 1996;21:609–20.
[52] Morgan HD, Watchus JA, Milgram NW, Fleming AS. The long lasting effects of electrical simulation of the medial preoptic area and medial amygdala on maternal behavior in female rats. Behav Brain Res 1999;99:61–73.
[53] Morgan MA, Pfaff DW. Effects of estrogen on activity and fear-related behaviors in mice. Horm Behav 2001;40:472–82.
[54] Morgan MA, Schulkin J, Pfaff DW. Estrogens and non-reproductive behaviors related to activity and fear. Neurosci Biobehav Rev 2004;28:55–63.
[55] Musatov S, Chen W, Pfaff DW, Kaplitt MG, Ogawa S. RNAi-mediated silencing of estrogen receptor in the ventromedial nucleus of hypothalamus abolishes female sexual behaviors. Proc Nat Acad Sci USA 2006;103:10456–60.
[56] Nomikos GG, Spyraki C. Influence of estrogen on spontaneous and diazepam-induced exploration of rats in an elevated plus maze. Neuropharmacology 1988;27:691–6.
[57] Ogawa S, Eng V, Taylor J, Lubahn DB, Korach KS, Pfaff DW. Roles of estrogen receptor alpha gene expression in reproduction-related behaviors in female mice. Endocrinology 1998;139:5070–81.
[58] Osterlund M, Kuiper GGJM, Gustafsson JA, Hurd YL. Differential distribution and regulation of estrogen receptor-alpha and -beta mRNA within the female rat brain. Mol Brain Res 1998;54:175–80.
[59] Pandaranandaka J, Poonyachoti S, Kalandakanond-Thongsong S. Anxiolytic property of estrogen related to the changes of the monoamine levels in various brain regions of ovariectomized rats. Physiol Behav 2006;87:828–35.
[60] Paxinos G, Watson C. The rat brain in stereotaxic coordinates. 4th ed. San Diego, CA: Academic Press; 1998.
[61] Pfaff DW. Estrogen and brain function. New York, NY: Springer-Verlag; 1980.
[62] Popik P, Vetulani J, Bisaga A, Van Ree JM. Recognition cue in the rat's social memory paradigm. J Basic Clin Physiol Pharmacol 1991;2:315–27.
[63] Rasia-Filho AA, Londero RG, Achaval M. Functional activities of the amygdala: an overview. J Psychiatry Neurosci 2000;25:14–23.
[64] Reyes-Guerrero G, Vazquez-Garcia M, Elias-Vinas D, Donatti-Albarran OA, Guevara-Guzman R. Effects of 17 ß-estradiol and extremely low-frequency electromagnetic fields on social recognition memory in female rats: a possible interaction? Brain Res 2006;1095:131–8.
[65] Richter K, Wolf G, Engelmann M. Social recognition memory requires two stages for protein synthesis in mice. Learn Mem 2005;12:407–13.
[66] Sawyer TF, Hengehold AK, Perez WA. Chemosensory and hormonal mediation of social memory in male-rats. Behav Neurosci 1984;98:908–13.
[67] Sclafani A. Neural pathways involved in ventromedial hypothalamic lesion syndrome in rat. J Comp Physiol Psychol 1971;77:70–96.
[68] Shipley M, Ennis M, Puche A. Olfactory system. In: Paxinos G, editor. The rat nervous system. London: Elsevier; 2004. p. 923–64.
[69] Spiteri T, Ågmo A. Modèles precliniques du désir sexuel. Sexologies 2006;15:241–9.
[70] Spiteri T, Ågmo A. Ovarian hormones modulate social recognition in female rats. Physiol Behav 2009;98:247–50.
[71] Spiteri T, Musatov S, Ogawa S, Ribeiro A, Pfaff DW, Ågmo A. Estrogen-induced sexual incentive motivation, proceptivity and receptivity depend on a functional estrogen receptor alpha in the ventromedial nucleus of the hypothalamus but not in the amygdala. Neuroendocrinology, in press.

[72] Spruijt BM, Vanhooff JARA, Gispen WH. Ethology and neurobiology of grooming behavior. Physiol Rev 1992;72:825–52.
[73] Swanson HH, Van De Poll NE, Van Pelt J. Influence of estrus cycle on heterosexual aggression in two strains of rats (S_3 and WEzob). Horm Behav 1982;16:395–403.
[74] Tang AC, Nakazawa M, Romeo RD, Reeb BC, Sisti H, Mcewen BS. Effects of long-term estrogen replacement on social investigation and social memory in ovariectomized C57BL/6 mice. Horm Behav 2005;47:350–7.
[75] Thor DH, Holloway WR. Social memory of the male laboratory rat. J Comp Physiol Psychol 1982;96:1000–6.
[76] Wade GN. Gonadal hormones and behavioral regulation of body-weight. Physiol Behav 1972;8:523–34.
[77] Walf AA, Ciriza I, Garcia-Segura LM, Frye CA. Antisense oligodeoxynucleotides for estrogen receptor-beta and alpha attenuate estradiol's modulation of affective and sexual behavior, respectively. Neuropsychopharmacology 2008;33:431–40.
[78] Walf AA, Frye CA. Antianxiety and antidepressive behavior produced by physiological estradiol regimen may be modulated by hypothalamic–pituitary–adrenal axis activity. Neuropsychopharmacology 2005;30: 1288–301.
[79] Walf AA, Koonce CJ, Frye CA. Estradiol or diarylpropionitrile administration to wild type, but not estrogen receptor beta knockout, mice enhances performance in the object recognition and object placement tasks. Neurobiol Learn Mem 2008;89:513–21.
[80] Yamamuro Y. Social behavior in laboratory rats: applications for psychoneuroethology studies. J Anim Sci 2006;77:386–94.
[81] Zhou J, Lee AW, Devidze N, Zhang QY, Kow LM, Pfaff DW. Histamine-induced excitatory responses in mouse ventromedial hypothalamic neurons: ionic mechanisms and estrogenic regulation. J Neurophysiol 2007;98:3143–52.
[82] Zimmerberg B, Farley MJ. Sex-differences in anxiety behavior in rats – role of gonadal-hormones. Physiol Behav 1993;54:1119–24.

Cellular/Molecular

Synaptic Tagging and Capture: Differential Role of Distinct Calcium/Calmodulin Kinases in Protein Synthesis-Dependent Long-Term Potentiation

Roger L. Redondo,[1] Hiroyuki Okuno,[2] Patrick A. Spooner,[1] Bruno G. Frenguelli,[3] Haruhiko Bito,[2] and Richard G. M. Morris[1]

[1]Centre for Cognitive and Neural Systems, University of Edinburgh, EH8 9JZ, Edinburgh, United Kingdom, [2]Department of Neurochemistry, University of Tokyo Graduate School of Medicine, Bunkyo-ku, Tokyo 113-0033, Japan, and [3]Department of Biological Sciences, University of Warwick, CV4 7AL, Coventry, United Kingdom

Weakly tetanized synapses in area CA1 of the hippocampus that ordinarily display long-term potentiation lasting ~3 h (called early-LTP) will maintain a longer-lasting change in efficacy (late-LTP) if the weak tetanization occurs shortly before or after strong tetanization of an independent, but convergent, set of synapses in CA1. The synaptic tagging and capture hypothesis explains this heterosynaptic influence on persistence in terms of a distinction between local mechanisms of synaptic tagging and cell-wide mechanisms responsible for the synthesis, distribution, and capture of plasticity-related proteins (PRPs). We now present evidence that distinct CaM kinase (CaMK) pathways serve a dissociable role in these mechanisms. Using a hippocampal brain-slice preparation that permits stable long-term recordings *in vitro* for >10 h and using hippocampal cultures to validate the differential drug effects on distinct CaMK pathways, we show that tag setting is blocked by the CaMK inhibitor KN-93 (2-[*N*-(2-hydroxyethyl)]-*N*-(4-methoxybenzenesulfonyl)amino-*N*-(4-chlorocinnamyl)-*N*-methylbenzylamine) that, at low concentration, is more selective for CaMKII. In contrast, the CaMK kinase inhibitor STO-609 [7*H*-benzimidazo(2,1-a)benz(de)isoquinoline-7-one-3-carboxylic acid] specifically limits the synthesis and/or availability of PRPs. Analytically powerful three-pathway protocols using sequential strong and weak tetanization in varying orders and test stimulation over long periods of time after LTP induction enable a pharmacological dissociation of these distinct roles of the CaMK pathways in late-LTP and so provide a novel framework for the molecular mechanisms by which synaptic potentiation, and possibly memories, become stabilized.

Introduction

Activity-dependent synaptic plasticity, such as long-term potentiation (LTP) (Bliss and Lomo, 1973), is widely thought to be involved in the encoding of new information during learning. Some forms of LTP decay to baseline over a short timescale (early-LTP), whereas others, notably late-LTP, show stable synaptic potentiation for much longer (Krug et al., 1984; Frey et al., 1988). The synaptic tagging and capture (STC) hypothesis of late-LTP (Frey and Morris, 1997) asserts that LTP involves the local "tagging" of synapses at the moment of induction, that tags capture diffusely transported "plasticity-related proteins" (PRPs) synthesized in the soma or local dendritic domains, and that tag–PRP interactions are essential for stabilization of potentiation. Various lines of evidence support this framework (Frey and Morris, 1997; Martin et al., 1997; Reymann and Frey, 2007), but important open questions concern the signal-transduction pathways involved in tag setting and PRP availability.

Because relevant molecular interactions are likely to take place over several hours after LTP induction, the short time course of most LTP experiments (1–3 h) may be insufficient to monitor all the processes involved in synaptic stabilization. We therefore developed long time course *in vitro* protocols that involve (1) an interaction of strong tetanization (that sets tags and upregulates PRP synthesis) and temporally adjacent weak tetanization (which only sets tags), and (2) the rapid onset and cessation of selective kinase inhibition at appropriate times. The successful cessation of inhibition requires both rapid drug washout (i.e., the drug does not permanently bind to its target) and rapid reversibility of the action of the drug (i.e., the effect of the drug is not sustained after washout such that the normal function of the inhibited target kinase is recoverable). This double reversibility is fundamental for the dissection of heterosynaptic interactions in plasticity. These protocols also involve three independent stimulus pathways to a common pool of hippocampal neurons and exceptional control of temperature and other parameters of slice physiology to enable routine stable long-term recordings and their measurement in excess of 12 h (see Fig. 1).

The present study explores the potentially differential roles of several Ca^{2+}/calmodulin-dependent protein kinase (CaMK)

Received June 10, 2009; revised Dec. 15, 2009; accepted Jan. 6, 2010.

This work was supported by grants from the Human Frontier Science Program (R.G.M.M., H.B.), Volkswagen Stiftung (R.G.M.M.), the U.K. Medical Research Council (R.G.M.M.), the Ministry of Education, Culture, Sports, Science and Technology and Ministry of Health, Labor, and Welfare of Japan (H.B., H.O.), the Takeda Foundation (H.B.), and the Yamada Science Foundation (H.B.). We thank Tobias Bonhoeffer, Rosalina Fonseca, Mark van Rossum, and members of the Laboratory for Cognitive Neuroscience in Edinburgh for discussion and Feruza Nuritova and Colin McKenzie for earlier data.

Correspondence should be addressed to R. G. M. Morris, Centre for Cognitive and Neural Systems, University of Edinburgh, 1 George Square, EH8 9JZ, Edinburgh, UK. E-mail: r.g.m.morris@ed.ac.uk.

DOI:10.1523/JNEUROSCI.3140-09.2010

 0270-6474/10/304981-09$15.00/0

family members in the duration of LTP. Although CaMKII regulates many neuronal functions (Erondu and Kennedy, 1985; Braun and Schulman, 1995; Yamauchi, 2005), various theoretical ideas and experimental lines of evidence suggest that its activation is necessary locally for the induction and expression of LTP at synapses of the CA3 to CA1 pathway of the hippocampus (Lisman and Goldring, 1988; Malenka et al., 1989; Malinow et al., 1989). A natural question is whether CaMKII may also possess a specific role in tag setting.

In contrast, in the cell soma, calcium entry triggers activation of CaMK kinase (CaMKK) activity that stimulates CaMKIV, a nuclear kinase capable of phosphorylating Ca^{2+}/cAMP-response element binding protein (CREB) that initiates the transcription of plasticity-related genes (Bito et al., 1996; Ho et al., 2000; Kang et al., 2001). Might the pathway involving CaMKK and CaMKIV be essential for the synthesis of PRPs? To test these ideas, we examined whether reversible inhibition of different CaM kinases can specifically interfere with either the setting of tags or the synthesis of PRPs (supplemental Fig. S1, available at www.jneurosci.org as supplemental material).

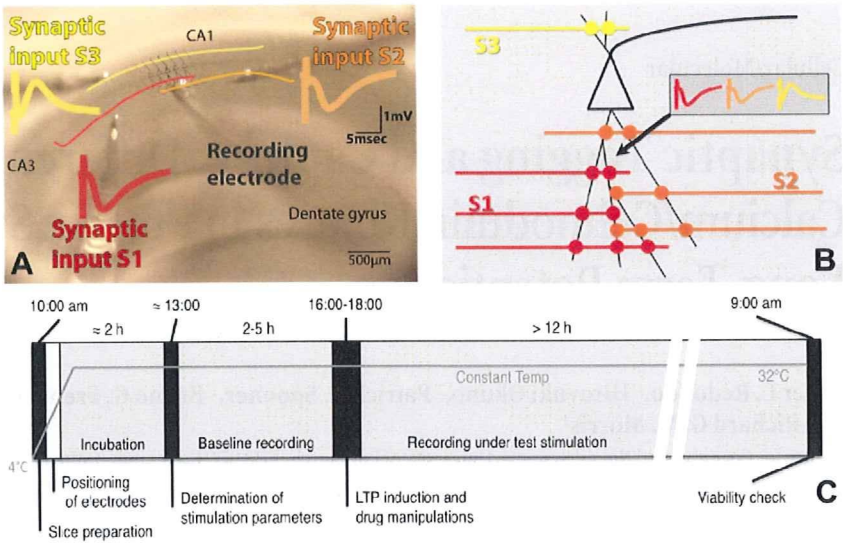

Figure 1. Experimental protocols. ***A***, The slice preparation with superimposed labels depicting the positioning of the electrodes. Color coding matches that used to identify the respective pathways throughout text. ***B***, Schematic representation depicting the independent but convergent inputs onto pyramidal cells in the CA1 used in these experiments. The recording electrode placed in the stratum radiatum of CA1 records three independent field EPSPs elicited by the activation of different populations of synapses onto the same cells. ***C***, Experimental protocol showing approximate phase lengths. Briefly, slices are cut in ice-cold aCSF and transferred to the recording chamber in which the electrodes are placed in position. Two hours of incubation allow the temperature to equalize to 32°C before input–output curves and paired-pulse stimulation tests are run to assess the optimal intensity of stimulation and confirm pathway independence, respectively. More than 2 h are still allowed to pass while baseline recordings are obtained before any drug or electrophysiological manipulations are introduced. After that, the setup returns to test-stimulation frequencies, and the experiment is allowed to develop overnight. An assessment of the viability of the slice is run the following morning (for more detailed information, see Materials and Methods).

Materials and Methods

The animals' care and maintenance and all experimental procedures were performed in accordance with United Kingdom Home Office regulations. Male Wistar rats ($n = 110$) aged 7–8 weeks were anesthetized with isoflurane and decapitated, and the brain was removed rapidly. Brain slices (400 μm) of the dorsal hippocampus were sectioned as described previously (Leutgeb et al., 2003). The hippocampal slices rested on top of eight layers of lens tissue paper (Whatman 105) placed on top of the hard surface of the slice chamber (BSC2 Scientific Systems Design; Digitimer). This ensured that the slice tissue was well soaked in the lens tissue paper while its surface remained exposed to air. All the artificial CSF (aCSF) volume held in the chamber was contained in the 2 cm wide × 2.5 cm long layers of lens tissue paper and amounted to 0.475 ml (i.e., dead volume in the chamber). All the experiments were run with the same low flow rate (0.4 ml/min) to minimize mechanical disruption of the recordings. Under these conditions, we calculate a full recycling of the aCSF every 71 s (i.e., 17 washes in 20 min). Although every drug has its own characteristics (i.e., site of action, affinity), we judged that 20 min would be enough to wash out the drugs used in these experiments. When drug washouts could be critical, alternative experiments were used to corroborate the interpretation of the result. The aCSF was prepared with the following concentrations (in mM): 124 NaCl, 3.7 KCl, 1.2 KH_2PO_4, 1.0 $MgSO_4$ (7 H_20), 2.5 $CaCl_2$, 24.6 $NaHCO_3$, and 10 D-glucose, final pH 7.4 ± 0.05. The full rig, including all the electrode holders, was heated to 32°C via the ETC system (University of Edinburgh), a procedure that prevents condensation droplets falling onto the interface chamber slices and so affecting neuronal stability.

One recording electrode, made from stainless steel rods (712700 A-M Systems), and three monopolar stainless steel electrodes (571000 A-M Systems) stimulating electrodes were positioned in CA1 (Fig. 1*A*). The slices rested for at least 2 h before preliminary recordings were taken, and no high-frequency stimulation was delivered until 5 h after dissection. The importance of this resting period for the stabilization of kinase phosphorylation levels has been emphasized previously (Ho et al., 2004; Sajikumar et al., 2005). Field EPSPs (fEPSPs) were recorded at 40–50% of the maximum amplitude obtained in an input–output curve. Test stimulation was 0.0067 Hz, 1 pulse per 150 s, resulting in one of the three channels being stimulated every 50 s (0.02 Hz). This low rate was chosen to allow the activity rates of kinases and other molecules to drop to a resting state between stimulation (Sajikumar et al., 2005). At this low rate of stimulation, hippocampal slices react more slowly to drugs such as anisomycin than at faster rates (Fonseca et al., 2006; Sajikumar et al., 2008). Also importantly, test stimulation activates NMDA receptors and the molecular cascades linked to it (Navakkode et al., 2007). Minimizing the impact of test stimulation is in the interest of recording stability (Schurr et al., 1986) as well as reproducibility of the data from experiment to experiment.

Data (fEPSP slope) was normalized to a baseline calculated over 60 min before the first tetanization. The "strong" tetanization protocol consisted of three trains of 100 pulses at 100 Hz delivered at 10 min intervals (300 pulses in total). The "weak" tetanization protocol was a theta burst consisting of four trains, at a 200 ms interval, consisting of five pulses at 100 Hz (20 pulses in total). Pathway independence was tested by using standard pair-pulse stimulation protocols that alternated between the two stimulating pathways placed in the stratum radiatum of CA1 (50 ms interpulse interval). The experiment proceeded provided this procedure failed to show paired-pulse facilitation (PPF). Normal PPF was detected when PPS was delivered to either of the two pathways as would be expected when the same presynaptic fibers are recruited by both pulses (data not shown). In addition to this control for pathway independence, the induction of LTP in one pathway fail to induce any LTP on the other two pathways in all our experiments. Pathway convergence is assumed from the limited area of sensitivity of the extracellular recording electrode, from the layered anatomy of the hippocampus, and from the observation of heterosynaptic plasticity dependent on intracellular processes (Schwartzkroin and Wester, 1975; Andersen et al., 1977; Frey and Morris, 1997).

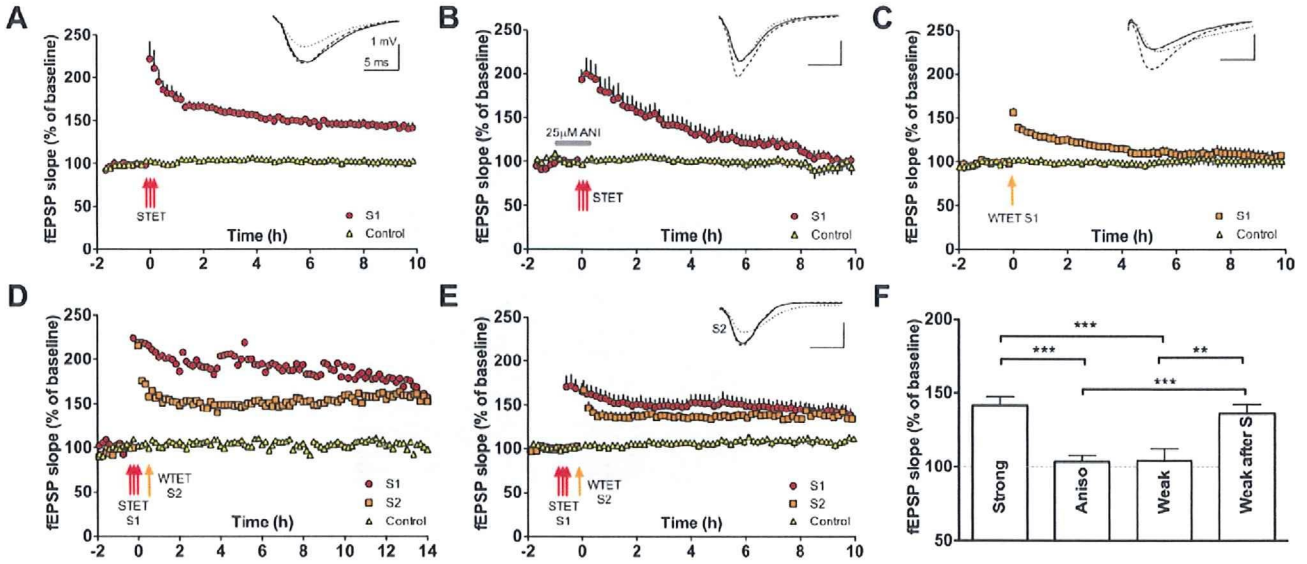

Figure 2. Synaptic tagging and capture in the stratum radiatum of CA1 pyramidal cells. ***A***, Strong tetanization (STET) (3 trains of 100 pulses at 100 Hz given 10 min apart) produces an increase in the synaptic response that lasts 10 h (late-LTP) relative to both the pretetanization baseline ($t = 8.0$, $p < 0.01$; red symbols) and a nontetanized control pathway ($t = 4.9$, $p < 0.01$; yellow symbols). This strongly induced LTP was stable over time (comparison of 2 and 10 h time points; $t = 2.0$, $p \geq 0.05$). The insets in each graph represent typical EPSP traces per stimulated input 30 min before (dotted line), 30 min after (broken line), and 10 h after (full line). Calibration: 1 mV, 5 ms ($n = 7$). ***B***, Late-LTP is not maintained when a strong tetanus is given in the presence of the protein synthesis blocker anisomycin. The potentiation declined to baseline after 10 h (S1 vs baseline; $t = 0.15$, $p \geq 0.05$; $n = 9$). ***C***, A weak tetanus (WTET) (4 trains of 5 pulses at 100 Hz given 200 ms apart) elicits LTP present at 2 h (S1 vs control pathway; $t = 4.3$, $p < 0.01$) that returns to baseline strength after 3 h (S1 vs control pathway; $t = 1$, $p \geq 0.05$; $n = 6$). ***D***, ***E***, Early-LTP (orange symbols) is rescued into late-LTP (S2 vs control pathway at 10 h; $t = 3.4$, $p \leq 0.01$) when one set of synapses receives the weak tetanus 20 min after another set of synapses onto the same population of pyramidal cells has received a strong tetanus (***D***, single experiment; ***E***, pooled data; $n = 8$). ***F***, Bar graph showing differences in the level of potentiation 10 h after stimulation between the four different conditions presented in ***A–E*** (one-way ANOVA, $F = 15.13$, $p < 0.001$). The change in synaptic efficacy remaining 10 h after the strong tetanization of a set of synapses is significantly higher than when the tetanization takes place under the presence of 25 μM anisomycin ($t = 5.45$, $p < 0.001$) and higher than the potentiation remaining after weak tetanization ($t = 4.53$, $p < 0.001$). In a similar way, the potentiation left after 10 h in a pathway weakly stimulated before strong tetanization was given to an independent but convergent set of synapses is greater than if the weak tetanization is given alone ($t = 3.92$, $p < 0.01$) or if a strong tetanus is given together with anisomycin ($t = 4.81$, $p < 0.001$). Error bars indicate SEM. $^{**}p < 0.01$; $^{***}p < 0.001$. Multiple *t* tests were comparisons done with Bonferroni's correction.

KN-93 (2-[*N*-(2-hydroxyethyl)]-*N*-(4-methoxybenzenesulfonyl)amino-*N*-(4-chlorocinnamyl)-*N*-methylbenzylamine), Myr-AIP (*N*-Myr-Lys-Lys-Ala-Leu-Arg-Arg-Gln-Glu-Ala-Val-Asp-Ala-Leu-OH), and KN-92 (2-[*N*-(4′-methoxybenzenesulfonyl)]amino-*N*-(4′-chlorophenyl)-2-propenyl-*N*-methylbenzylamine phosphate) were obtained from Calbiochem, anisomycin and D-AP-5 were from Sigma, and STO-609 [7*H*-benzimidazo(2,1-a)benz(de)isoquinoline-7-one-3-carboxylic acid] was from Tocris Bioscience.

The average values of the slope function of the fEPSP (millivolts per milliseconds) for each time point were analyzed using paired (within-group) and unpaired (between-group) *t* tests; $p < 0.05$ was considered as statistically significant, but we show more exacting levels of significance in many cases. Parametric tests were used because the data conformed to a Gaussian distribution, but analysis using nonparametric tests (Mann–Whitney and Wilcoxon's tests) supported the same conclusions. To measure the stability of late-LTP, we compared the absolute level of potentiation relative to the baseline 2 h after its induction with the level remaining after 10 h. This measure distinguishes stability and amplitude in a manner that is not usually considered. Specifically, it distinguishes between "stable late-LTP" and "decaying LTP that still shows potentiation at the end of the experiment" because the latter may arise if there is strong initial expression of LTP. We hope that this measure clarifies the difference between strength and persistence of LTP.

Hippocampal dissociated cultures were prepared from neonatal Wistar rats and cultured on coverslips as described previously (Bito et al., 1996; Kawashima et al., 2009). At 20–21 d *in vitro*, at which synaptic network in the culture was well developed, neurons were silenced with 2 μM TTX for 2 h and treated with various concentrations of kinase inhibitors (KN-93 or STO-609 in 0.1% DMSO) for 30 min in Tyrode's solution (in mM: 124 NaCl, 2.5 KCl, 1.0 NaH_2PO_4, 2.0 $CaCl_2$, 2.0 $MgCl_2$, 24.6 $NaHCO_3$, 30 D-glucose, and 20 HEPES, pH 7.4). The cultures were then stimulated with 10 μM glutamate/100 μM glycine/1 μM TTX in 0 Mg^{2+} Tyrode's solution for 3 min in the presence of the inhibitors. After stimulation, neurons were immediately fixed in chilled methanol for 5 min, followed by ice-cold 4% paraformaldehyde/4% sucrose/PBS for 5 min.

Immunocytochemistry was performed essentially as described previously (Kawashima et al., 2009). Briefly, the fixed cells were washed, permeabilized, and incubated in a blocking solution (3% BSA/0.3% Triton X-100/PBS) with a phosphatase inhibitor cocktail (PhosSTOP; Roche). The cells were then reacted with primary antibodies in the blocking solution. The primary antibodies used were anti-phosphorylated-CREB (pCREB) [rabbit monoclonal antibody (mAb); Epitomics] and anti-MAP2 (mouse mAb; Sigma) or anti-pCaMKII (rabbit polyclonal antibody; Promega) and anti-CaMKIIα (mouse mAb; Invitrogen). After the wash, the primary antibodies were labeled with anti-mouse AlexaFluor488-conjugated and anti-rabbit AlexaFluor594-conjugated secondary antibodies. The cells were then washed, stained with 4′,6′-diamidino-2-phenylindole (DAPI), and mounted on slides.

Fluorescence images were acquired using a confocal laser scanning microscopy or an EM-CCD camera mounted on an inverted microscope. To obtain two-dimensional images, a *z*-stack of multiple confocal section images were acquired using an LSM510 META confocal laser microscope (Carl Zeiss), and then the stack data were projected into single planes by a summation algorithm. The projected images were color coded and shown. To quantify fluorescent pixel intensities, single-plane images were directly acquired using an EM-CCD camera (Andor) mounted on an inverted microscope (IX81; Olympus), to take advantage of the higher sensitivity and dynamic range of the camera. For quantification, regions of interest (ROIs) were set on neuronal nuclei, which were defined by DAPI and MAP2 staining, for pCREB immunoreactivity (n = 89–154 neurons per condition), and on dendritic spines defined based on total CaMKIIα immunoreactivity for pCaMKII (n = 127–203 spines from 9–12 neurons). Average intensity in each ROI was calculated using the

MetaMorph software (Universal Imaging Corporation), and dose-dependent curves were drawn using the Prism software (GraphPad Software). The values under TTX condition and stimulation without drugs (DMSO only) were defined as basal (0%) and maximum (100%) activities, respectively. The image analyses were done in a blind manner.

Results

Synaptic tagging and capture

Conventional experiments examining late-LTP relative to a nontetanized baseline cannot, alone, isolate the putatively distinct roles played by different signal-transduction pathways in synaptic tagging, the availability of PRPs, or the putative capture process. Two-pathway experiments deploying what we shall call "weak-before-strong" and "strong-before-weak" protocols, in which weak and strong tetanization are given sequentially to two independent pathways, are essential to examine the dissociations that are central to this study. Ideally, to perform long experiments in which two independent pathways are tetanized at some point, it is desirable to have a three-pathway configuration with a third nontetanized pathway to monitor the overall stability of the slice preparation (Fig. 1). We incorporated this to enable potentiated pathways to be compared with the control pathway at various time points rather than only make comparisons to pretetanus baselines. We began by establishing that our tetanization protocols are successful in producing late-LTP that is exceptionally stable over time.

LTP lasting >10 h with an absolute level of ~142% (at 10 h) relative to both the pretetanization baseline ($p < 0.01$) and higher than a nontetanized control pathway ($p < 0.01$) was routinely obtained after strong tetanization (Fig. 2*A*). This persistent late-LTP was sensitive to the presence of the protein synthesis blocker anisomycin at induction; in addition to displaying fEPSP decay over time with anisomycin, there was no difference between fEPSP slope at 10 h after tetanus (S1) and the pretetanus baseline ($p > 0.05$) nor between S1 and the control pathway at 10 h after tetanus ($p \geq 0.05$). Using our novel "stability" measure (described in Materials and Methods), the within-pathway decline in the level of potentiation in S1 from 2 to 10 h was significant ($p < 0.01$) (Fig. 2*B*). The NMDA receptor antagonist D-AP-5 (25 μM) blocked LTP induction (S1 relative to control; $p > 0.05$). After washout and 1 h after the previous tetanus, a second strong tetanization was delivered to confirm the reversibility of the NMDA receptor block, and, under these conditions, late-LTP could be induced ($p < 0.05$) (supplemental Fig. S2, available at www.jneurosci.org as supplemental material).

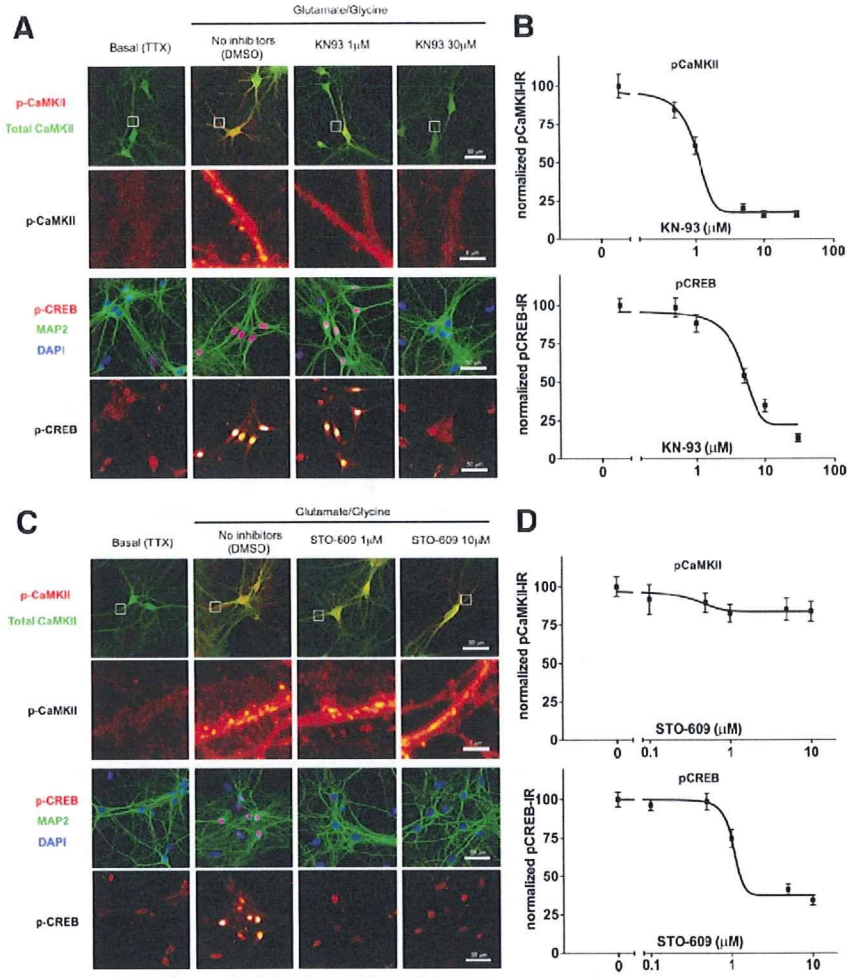

Figure 3. Dose-related effects of KN-93 and STO-609 on phosphorylation of CaMKII and CREB. ***A***, Top, Effects of kinase inhibitors on pCaMKII (top rows) and on pCREB (bottom rows) in dissociated hippocampal culture. Neurons were stimulated with bath application of glutamate/glycine in the presence of KN-93. pCaMKII immunoreactivity in dendritic spines was measured for quantification. Framed areas in the top row were expanded and pCaMKII channel was shown at the bottom in a pseudocolor scale. pCREB immunoreactivity was quantified in neuronal nuclei that were identified with MAP2 and DAPI staining. The pCREB channel was separately shown in a pseudocolor scale below. ***B***, Differential dose responses of KN-93 on distinct CaMK pathways in culture neurons. Top, Effects of KN-93 on CaMKII autophosphorylation at Thr-286. Immunoreactivity (IR) for pCaMKII was quantified in dendritic spines and displayed as a function of KN-93 concentration. The ordinate represents basal (no stimulation, 0%) to maximum (stimulated without inhibitors, 100%) activities. Bottom, Effects of KN-93 on CREB phosphorylation at Ser-133. Suppression of pCREB immunoreactivity in the neuronal nuclei was displayed. Note greater sensitivity of KN-93 for CaMKII. ***C***, Effects of STO-609 on pCaMKII and on pCREB in dissociated hippocampal culture. Neurons were stimulated with bath application of glutamate/glycine in the presence of STO-609. pCaMKII immunoreactivity in dendritic spines was measured for quantification. Framed areas in the top row were expanded and pCaMKII channel was shown at the bottom in a pseudocolor scale. pCREB immunoreactivity was quantified in neuronal nuclei that were identified with MAP2 and DAPI staining. The pCREB channel was separately shown in a pseudocolor scale below. ***D***, Differential dose responses of STO-609 on distinct CaMK pathways in culture neurons. Top, Effects of STO-609 on CaMKII autophosphorylation at Thr-286. Bottom, Effects of STO-609 on CREB phosphorylation at Ser-133. Error bars indicate SEM.

Thus, strong tetanization induced an NMDA receptor-dependent, anisomycin-sensitive late-LTP. Conversely, potentiation induced by weak tetanization was clearly present at 2 h (25% above baseline; $p < 0.01$), but this early-LTP declined within 6 h and was absent after 10 h ($p > 0.05$, relative to control) (Fig. 2*C*). Using our measure of LTP stability over time, comparison of the 2 and 10 h time points showed a significant decline in the weakly tetanized synapses ($p < 0.05$).

To demonstrate STC, the strong tetanus protocol was then given to pathway S1, and, 20 min after the last 100 Hz train, a weak tetanus was applied to a second independent but conver-

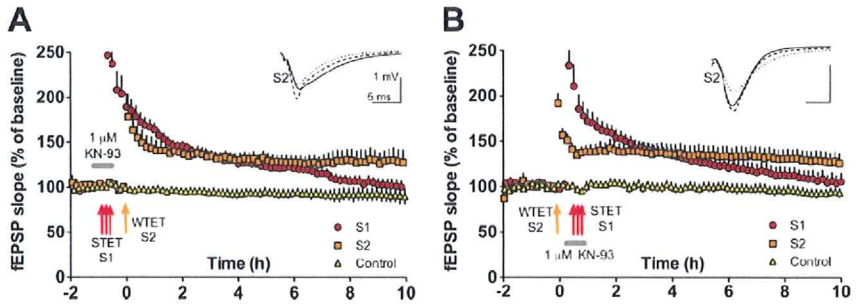

Figure 4. KN-93 dissects a role for CaMKII in a synapse-specific process necessary for late-LTP. ***A***, Strong tetanization (STET) in the presence of 1 μM KN-93 (pathway S1) induces LTP that decays to baseline over 10 h (S1 vs control pathway, $t = 1.7, p \geq 0.05$; red symbols), whereas an independent set of weakly tetanized (WTET) synapses (S2; orange symbols) successfully shows stable potentiation for 10 h after tetanus (S2 relative to baseline at 10 h after tetanus, $t = 3, p \leq 0.05$; S2 at 2 vs 10 h, $t = 1.2, p \geq 0.05$; $n = 8$). ***B***, In a weak-before-strong protocol, early-LTP is still rescued to late-LTP (S2 vs control pathway, $t = 3.2, p \leq 0.05$), although late-LTP fails to be maintained in those synapses tetanized in the presence of 1 μM KN-93 (S1 vs control pathway, $t = 1.4$, $p \geq 0.05$; S1 at 2 vs 10 h, $t = 4.7, p \leq 0.01$; $n = 7$). Error bars indicate SEM. Symbols as in Figure 2.

gent pathway S2 (strong-before-weak protocol). In a single representative experiment, late-LTP was observed on both pathways lasting >14 h (Fig. 2*D*). The group data of a series of experiments ($n = 8$) revealed that pathway S2 maintained its potentiated state for at least 10 h. This was shown by comparing S2 with the third, control pathway ($p \leq 0.01$) and by establishing stability over the 2–10 h posttetanization time period (S2 at 2 vs 10 h, $p \geq 0.05$) (Fig. 2*E*). This stable late-LTP on S2 also differed from that seen on weakly tetanized pathways in slices that did not receive heterosynaptic strong stimulation (compare S2 in Fig. 2*E* with *C* at 10 h: $t = 3.4$, $p < 0.05$).

These results confirm previous findings (Frey and Morris, 1997, 1998a) and extend them through our use of three pathways and a monitoring time after LTP of >8 h, additional features essential for the later phases of experimentation.

Differential sensitivity of phosphorylated CaMKII and CREB to varying concentrations of KN-93 and STO-609

The CaMK inhibitor KN-93 has a broad spectrum of specificity for inhibiting CaM kinases, but the dose–response profile differs between CaMK subtypes. To verify the sensitivity of both CaMKII-mediated and CaMKK/CaMKIV-mediated phosphorylation processes to KN-93, cultured hippocampal neurons were exposed to robust glutamate-induced stimulation of phosphorylation, and we measured immunoreactivities for both pCaMKII (as a readout of CaMKII activity) and pCREB (as a functional readout of CaMKIV activation), in the presence of graded concentrations of KN-93 (Fig. 3*A*). Both pCaMKII and pCREB were blocked at a high concentration (e.g., 30 μM). The dose–response relation for inhibition of pCREB was rightward shifted relative to pCaMKII inhibition (Fig. 3*B*), consistent with the ideas that (1) CaMKII phosphorylation is more sensitive to KN-93, and (2) a higher concentration of KN-93 should be necessary to fully block PRP synthesis and availability. It is important to note that a low (1 μM) concentration of KN-93 has been shown previously to be sufficient to impair synaptic plasticity in brain slices (Hansel et al., 2006). CaMKII, with a K_i of 370 nM (Sumi et al., 1991), should be effectively blocked at this concentration, whereas the activity of other CaM kinases, such as CaMKIV, would be far less potently inhibited (Ishida et al., 1995).

In contrast, immunocytochemical assays using cultured neurons revealed that high concentrations of STO-609 (>1 μM) are capable of blocking phosphorylation of CREB, because CaMKK lies upstream of the CREB kinase CaMKIV but does not interfering with CaMKII phosphorylation (Fig. 3*C*,*D*).

KN-93 at 1 μM blocks late-LTP but allows a separate and weakly tetanized pathway to display late-LTP

Using the critical strong-before-weak protocol, KN-93 (1 μM) was applied during the strong tetanization of one pathway (S1, to block late-LTP) and washed out, and, 20 min later, weak tetanization was delivered to pathway S2. KN-93 completely blocked late-LTP on pathway S1 (compare pretetanus baseline at 10 h and control pathway in Fig. 4*A*, $p > 0.05$). In contrast, pathway S2 weakly stimulated 20 min after KN-93 washout maintained late-LTP for at least 10 h (Fig. 4*A*, $p < 0.05$) and was stable from 2 to 10 h ($p > 0.05$). The level of potentiation in the two pathways "crossed over." This is a critical observation, because it implies that PRPs must have been made available to synapses of the S2 pathway. Because S2 was weakly tetanized, the PRPs were likely upregulated by the strong tetanization of pathway S1. Given that pathway S1 decayed to baseline, it follows that 1 μM KN-93 must have selectively blocked a process critical for late-LTP but distinct from PRP availability, namely tag setting.

We confirmed these findings using the alternative weak-before-strong protocol. The weakly tetanized pathway (S2) showed sustained late-LTP over 10 h ($p < 0.05$), despite the decay to baseline (and crossover) of the potentiation induced by the later strong tetanization in the presence of KN-93 of the S1 pathway (compare baseline and control pathway in Fig. 4*B*, $p > 0.05$). Together, these experiments suggest that CaMKII, being sensitive to lower concentrations of KN-93, might play a major role in tag setting, whereas its role in the regulation of PRP availability might be more limited.

This suggestion relies on the actions of a general CaMK inhibitor that was used at a low dose at which it preferentially inhibits CaMKII. To strengthen the view of a specific role for CaMKII in tag setting, we also tested the effect of a myristoylated, cell-permeant, form of a CaMKII-selective inhibitory peptide, AIP (Ishida et al., 1995). We first confirmed that Myr-AIP can strongly inhibit pCaMKII formation in cultured neurons in the absence of any effect on pCREB (supplemental Fig. S3*A*,*B*, available at www.jneurosci.org as supplemental material). Next, using a standard strong-before-weak STC protocol, we tested whether the rescue of early-LTP into late-LTP (supplemental Fig. S3*C*, available at www.jneurosci.org as supplemental material) would be compromised by the presence of 5 μM Myr-AIP during early-LTP induction. Myr-AIP was bath applied during the weak tetanization of S2. In keeping with our previous results with a low concentration of KN-93, pathway S2 failed to show late-LTP [compare with baseline in supplemental Fig. S3*D* (available at www.jneurosci.org as supplemental material), $p > 0.05$]. We also note that early-LTP is diminished in the presence of Myr-AIP, consistent with previous results (Sanhueza et al., 2007). This indicates that Myr-AIP blocked the ability of PRPs generated in pathway S1 to convert a subsequent early-LTP in S2 into late-LTP, i.e., it compromised tag setting. Together, these data

indicate that CaMKII phosphorylation specifically mediates tag setting.

STO-609 blocks late-LTP but permits a pathway tetanized in its presence to display late-LTP provided an independent pathway is tetanized strongly

The CaMKK–CaMKIV pathway mediates CREB phosphorylation and neuronal activity gene transcription (Bito et al., 1996; Ho et al., 2000; Kang et al., 2001). However, it has not been formally addressed before whether a CaMKK–CaMKIV–pCREB pathway might contribute to the regulation of PRP availability. Three-pathway protocols were then used to examine the contribution to late-LTP the CaMKK–CaMKIV-dependent pathway. We used the CaMKK inhibitor STO-609 (Tokumitsu et al., 2002). We first confirmed that STO-609 (5 μM) blocks the late phase of LTP (S1 compared with baseline in Fig. 5*A*, $p > 0.05$). Because STO-609 has little effect on CaMKII activity (Fig. 3*C*,*D*), our perspective is that STO-609 may block late-LTP through a selective effect on the synthesis or distribution of PRPs. To test this, we therefore made the drug present during the weak tetanization of pathway S2 and then washed it out before strong tetanization was applied to pathway S1. In this weak-before-strong protocol, we observed a rescue of early-LTP into late-LTP on the weakly stimulated pathway S2 (compared with baseline in Fig. 5*B*, $p < 0.05$). This was not attributable to some cryptic "potentiating" effect of STO-609, because giving this drug during weak tetanization of a single pathway was without effect on its decay to baseline (Fig. 5*C*, $p > 0.05$). Thus, STO-609 blocks late-LTP without effect on tag setting. The STC theory holds that it must be attributable to limiting the synthesis or availability of PRPs via inhibition of the CaMKK-dependent pathway. We tested this directly using a standard "strong-before-strong" STC protocol in which STO-609 was present during the first strong tetanization but not during the second one. In support of our interpretation, pathway S1 showed late-LTP (compared with baseline in Fig. 5*D*, $p < 0.01$). Supplemental experiments using a weak-before-strong protocol with STO-609 present during strong tetanization revealed no late-LTP on the weakly stimulated pathway, also in keeping with this interpretation [supplemental Fig. S4 (available at www.jneurosci.org as supplemental material), $p > 0.05$].

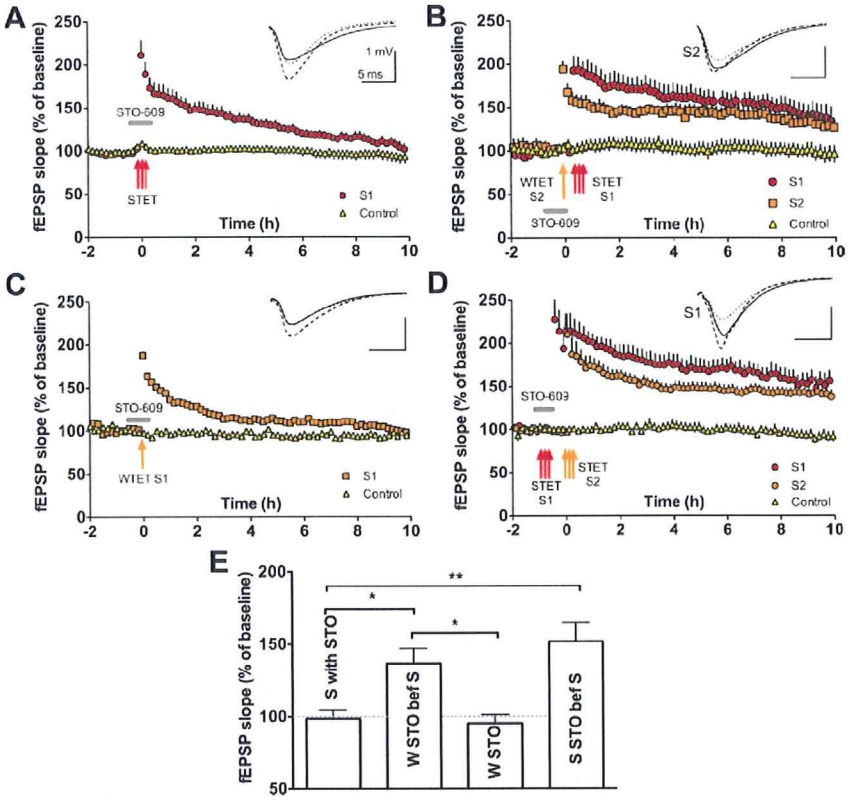

Figure 5. STO-609 dissects a role for CaMKK in a cell-wide process necessary for late-LTP. ***A***, The CaMKK inhibitor STO-609 (5 μM) present at the time of induction blocks late-LTP (S1 vs control pathway at 10 h, $t = 1$, $p \geq 0.05$; $n = 6$). ***B***, Weakly tetanized synapses show late-LTP when STO-609 is applied during the weak tetanus and then removed before strong stimulation is delivered to an independent pathway (S2 vs control pathway, $t = 2.7$, $p \leq 0.05$; stable from 2 to 10 h, $t = 2$, $p \geq 0.05$; $n = 5$). ***C***, STO-609 has no effect on a weakly tetanized pathway S1 (S1 vs baseline at 10 h, $t = 0.65$, $p > 0.05$; $n = 6$). ***D***, In a strong-before-strong protocol, STO-609 given tetanization to S1 does not prevent that pathway showing late-LTP if, after drug washout, strong tetanization is delivered to a second S2 pathway (S1 vs baseline at 10 h, $t = 5$, $p < 0.01$; $n = 6$). ***E***, Bar graph showing differences in the level of potentiation 10 h after stimulation between the four different conditions presented in ***A–D*** (one-way ANOVA, $F = 9.82$, $p < 0.001$). Strong tetanization in the presence of STO-609 fails to produce late-LTP, whereas sets of synapses that received weak tetanization in the presence of STO-609 succeed in maintaining late-LTP if within 20 min a strong tetanus is applied to a second convergent pathway (strong with STO-609 compared with weak tetanus with STO-609 rescued by a strong tetanus, $t = 2.87$, $p < 0.05$). This late-LTP is larger than when no strong tetanus accompanies the weak stimulation (weak tetanus with STO-609 rescued by a strong tetanus compared with weak with STO-609 alone, $t = 3.11$, $p < 0.05$). The effect of STO-609 on a strongly tetanized pathway can be prevented by a strong tetanus to another set of synapses (strong tetanus with STO-609 compared with strong tetanus with STO-609 rescued by a strong tetanus, $t = 4.17$, $p < 0.01$). Error bars indicate SEM. $^*p < 0.05$; $^{**}p < 0.01$. Symbols as in Figure 2. STET, Strong tetanization; WTET, weak tetanization.

KN-93 at 10 μM has less selectivity and blocks both tag setting and PRPs

We conducted three additional control studies. First, our cell-culture data indicate that KN-93 blocks the phosphorylation of CREB at high but not low concentrations (Fig. 3*A*,*B*). Accordingly, we can make the additional prediction that the relative selectivity of a 1 μM concentration of KN-93 on tag setting would be lost if the concentration was increased to 10 μM. Specifically, a higher concentration of KN-93 should block both tag setting and PRP synthesis and availability. Using the same strong-before-weak protocol as the one described in Figure 4, 10 μM KN-93 still blocked late-LTP of the strongly stimulated pathway S1 (compare baseline and control pathway in Fig. 6*A*, $p > 0.05$), but pathway S2 that was weakly tetanized after KN-93 washout now also failed to maintain its potentiation (compare baseline and control pathway in Fig. 6*A*, $p > 0.05$). The interpretation of this result relies on the complete washout of KN-93 by the time the weak tetanus is delivered. As explained in Materials and Methods, our setup allows for >15 washes of the aCSF volume in the experimental chamber between the removal of the drug and the weak tetanization. So as not to rely only on the findings of Figure 4*C*, the same pattern of results was obtained using the weak-before-strong protocol, in which the weak tetanization is delivered before the application of KN-93 (10 μM KN-93 blocked late-LTP in both the strong and weakly tetanized pathways) (Fig. 6*B*, $p > 0.05$). A parsimonious explanation for this would be the contribution of

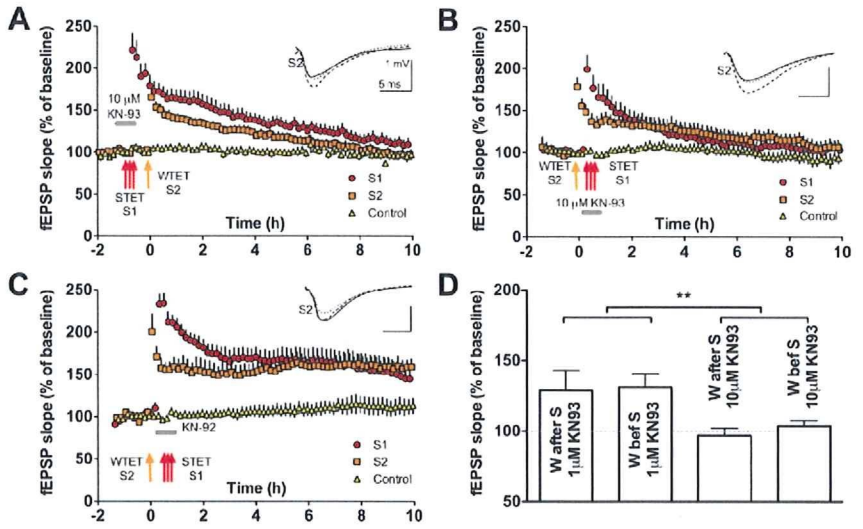

Figure 6. A higher concentration of KN-93 has less selective effects than a lower concentration. ***A***, ***B***, Higher concentrations of KN-93 fail to dissociate synapse-specific and cell-wide processes in late-LTP, in contrast to data in Figure 2 with 1 μM KN-93. ***A***, A weakly stimulated pathway (S2) failed to show late-LTP (S2 vs control 10 h, $t = 0.1$, $p \geq 0.05$) when the stimulation was given 20 min after a strong tetanus to S1 if the higher concentration of 10 μM KN-93 was present during LTP induction. The strongly stimulated pathway also fails to show late-LTP (S1 vs control 10 h, $t = 1.4$, $p \geq 0.05$; $n = 9$). ***B***, The rescue of early-LTP into late-LTP is also not seen in S2 (S2 vs control 10 h, $t = 1.7$, $p \geq 0.05$) if tetanization is given when 10 μM KN-93 is present during S1. S1 also fails to maintain late-LTP (S1 vs control 10 h, $t = 0.9$, $p \geq 0.05$; $n = 7$). ***C***, The rescue of early-LTP into late-LTP in a weakly tetanized pathway (S2) is seen even if S1 strong tetanization is delivered when KN-92 is present (S2 vs control 10 h after tetanus, $t = 3.5$, $p < 0.01$; $n = 5$). ***D***, Bar graph showing differences in the level of potentiation 10 h after stimulation between the two concentrations of KN-93 used in Figures 4 and 6 (two-way ANOVA, $F = 7.7$, $p < 0.01$). The order of stimulation and drug application had no effect ($F = 0.14$, $p > 0.05$). Error bars indicate SEM. $^{**}p < 0.01$. Symbols as in Figure 2. STET, Strong tetanization; WTET, weak tetanization.

KN-93-sensitive CaM kinase(s) distinct from CaMKII, such as the CaMKK–CaMKIV pathway, with respect to PRP availability.

The second control study is for nonspecific effects of KN-93. We did this using the inactive analog KN-92 (10 μM). Using a weak-before-strong protocol, KN-92 did not prevent the rescue of early-LTP on a weakly tetanized pathway S2 when given in the presence of strong tetanization on S1 (Fig. 6*C*, $p < 0.01$).

Third, we checked that KN-93 would still block tag setting at a high concentration. In previous work (Sajikumar and Frey, 2007), a strong-before-strong protocol was used to examine the effect of KN-62 (1-[*N*,*O*-bis(5-isoquinolinesulphonyl)-*N*-methyl-L-tyrosyl]-4-phenylpiperazine) (an alternative inhibitor of CaM kinases) on late-LTP, finding evidence for a role in tag setting. The strong-before-strong protocol is sufficient to identify a role in tag setting, although not as analytically powerful as the strong-before-weak protocols. Nonetheless, we observed that, if present at the time of induction, a 10 μM concentration of KN-93 blocked late-LTP at 10 h [pathway S2 compared with baseline in supplemental Fig. S5*A* (available at www.jneurosci.org as supplemental material), $p > 0.05$] but had no effect on the induction of LTP on a pathway tetanized 20 min earlier [pathway S1 compared with baseline in Fig. S5*A* (available at www.jneurosci.org as supplemental material), $p < 0.01$]. In separate experiments, the order was reversed and the same dose of KN-93 was present during the first tetanization but was then washed out. Late-LTP on the pathway tetanized under 10 μM KN-93 failed to show any potentiation 10 h after tetanus when compared with a control baseline [pathway S1 in supplemental Fig. S5*B* (available at www.jneurosci.org as supplemental material), $p > 0.05$]. However, after 20 min of aCSF flow into the chamber that successfully washed out KN-93, tetanization of the second pathway induced robust late-LTP lasting 10 h [pathway S2 in supplemental Fig. S5*B* (available at www.jneurosci.org as supplemental material), $p < 0.01$]. Also, KN-92 did not impair late-LTP if present during strong tetanization [compare baseline and control pathway in supplemental Fig. S5*C* (available at www.jneurosci.org as supplemental material), $p < 0.01$].

Discussion

These experiments have identified dissociable roles specific for distinct CaM kinase pathways in the persistence of synaptic potentiation, and they provide new molecular insights on the requirement for synapse-specific and cell-wide mechanisms mediating late-LTP. Our findings emerge from our use of long time course three-pathway protocols (i.e., two pathways tetanized in weak-before-strong and strong-before-weak modes, with a third nontetanized control pathway), which were readily combined with fast wash-in/washout pharmacological treatments. First, we confirm previous observations (Frey and Morris, 1997; Fonseca et al., 2004) that early-LTP induced at one set of synapses can be rescued into late-LTP if, within a short time window (Frey and Morris, 1998a), late-LTP is induced at another set of synapses in the same CA1 neuronal population (Fig. 2). Second, cell-biological data reveals differential concentration-dependent effects of KN-93 and STO-609 on two complementary requirements for the maintenance of LTP, with 1 μM KN-93 having specific effects on phosphorylation of CAMKII, whereas higher concentrations also affected pCREB, with STO-609 having no affect on pCaMKII (Fig. 3). Third, the low concentration of KN-93 selectively interrupted a pathway-specific tagging process but spared the availability of PRPs, as analytically revealed by successful late-LTP after weak tetanization of a second independent pathway (Fig. 4). A separate CaMKII inhibitor, Myr-AIP, had similar actions (supplemental Fig. S3, available at www.jneurosci.org as supplemental material). Fourth, STO-609 was shown to block late-LTP but to spare the setting of synaptic tags (Fig. 5). Fifth, consistent with dose–response profile shown in the cell-culture immunocytochemistry, we observed that a higher concentration of KN-93 blocked late-LTP but did so by both blocking tagging and other cell-wide mechanisms (Fig. 6), a result that builds on previous work with KN-62 (Sajikumar et al., 2007).

The synaptic tagging and capture hypothesis provides the key concepts that are central to our analysis of the rescue of early-LTP into late-LTP (Frey and Morris, 1998b). Indeed, this hypothesis asserts and predicts two requirements for long-term changes in synaptic efficacy: (1) the local setting of tags at stimulated synapses, and (2) the cell-wide or dendritic-domain-wide availability of PRPs that can be captured by the tags and so enable mechanisms responsible for the stabilization of potentiation (Reymann and Frey, 2007). However, the signal transduction pathways mediating these two requirements have remained unclear. Amid the potentially numerous molecular players and complex interactions involved in these processes, some may be

required for both tag setting and PRP availability [e.g., activation of NMDA receptors (O'Carroll and Morris, 2004)]. Other molecules (or molecular states, such as phosphorylation) may only be necessary for tag setting and yet others only for PRP synthesis and/or their availability (supplemental Fig. S1, available at www.jneurosci.org as supplemental material). Our experiments identify a dissociable molecular cascade within the CaM kinase pathways for both tag setting and PRP supply.

Specific targeting of tag setting using a low concentration of KN-93 and of PRP synthesis using STO-609

CaMKII is a broad-range kinase that regulates many neuronal functions (Erondu and Kennedy, 1985; Braun and Schulman, 1995; Yamauchi, 2005). In the CA3 to CA1 Schaffer-collateral pathway of the hippocampus, CaMKII activation by Ca^{2+}/CaM is required at the time of LTP induction (Malenka et al., 1989) and, as shown recently, remains necessary during the maintenance of LTP (Sanhueza et al., 2007). Compelling evidence indicates that a dodecameric holoenzyme is activated by intersubunit phosphorylation in the presence of calcium/calmodulin (Miller and Kennedy, 1986; Hanson et al., 1994). According to this model, during a robust Ca^{2+} signal, the binding of calmodulin to each subunit unmasks the kinase domain by repelling the autoinhibitory domain of CaMKII but also exposing a threonine 286 site (Thr-286) in the adjacent subunit. The subsequent phosphorylation of Thr-286 then generates an autonomous kinase activity and also increases the affinity for calmodulin and creating a state in which calmodulin is transiently trapped by CaMKII even shortly after the end of a Ca^{2+} transient (Meyer et al., 1992). It has been proposed that this property may enable active CaMKII to translocate into the spine (Zhang et al., 2008) and for autophosphorylated CaMKII to act as a switch capable of maintaining changes in synapse efficacy (Lisman and Goldring, 1988; Lisman and Zhabotinsky, 2001; Miller et al., 2005). This switch could, in principle, also participate in tag setting and/or the local capture of available PRPs (Sajikumar et al., 2007).

To secure definitive evidence for these ideas, we developed a long time course three-pathway slice recording protocol and then conducted robust differential CaMK pharmacological experiments whose aim was to experimentally dissociate tag setting and PRP supply. Our key observations are that (1) a low dose of KN-93, which interferes with the phosphorylation of CaMKII in cell culture but spares most CREB phosphorylation, has the effect of specifically inhibiting tag setting while allowing PRP availability heterosynaptically, whereas (2) STO-609 selectively affects CREB phosphorylation but not pCaMKII and blocks PRP availability without affecting tag setting.

The value of 10 h experiments and fast-reversible pharmacological interventions

The present findings underwrite the value of allowing newly prepared brain slices, subject to minimal test stimulation, to stabilize for at least 4 h before tetanization, as long recommended by the Frey group in Magdeburg, Germany. Biochemical data suggest that it can take hours before kinase activation levels stabilize after slice preparation (Ho et al., 2004) and that low frequencies of test stimulation cause minimal interference with PRP availability (Fonseca et al., 2006). We also recorded for much longer periods than is typical in many LTP experiments, making it desirable, if not essential, to have a third nontetanized control pathway. Our data provide additional indications that the dynamic interactions set in train by tetanization continue for several hours (e.g., in Fig. 4*B*, the crossover of the strong and weakly tetanized pathways takes place over a period from 2 to 6 h after tetanization, and the strongly tetanized pathway does not decay to baseline until 8–10 h have elapsed). These points may seem merely methodological but, in our view, have been critical to dissecting the differential role of distinct CaM kinases with respect to synaptic tagging and capture.

It is unfortunate that we could not use brain slices from mice subject to gene targeting of the calcium/calmodulin pathway (Giese et al., 1998). The reason is that the dissociation of tag setting and PRP synthesis requires the differential inhibition of different components of CaMK pathways to be rapidly reversible. A pharmacological approach was essential, although we anticipate that our approach could be complemented by observations on suitable genetic reporter mice in the future.

Multiple dissociable CaMK pathways contribute to STC

Despite a large body of work on activity-dependent transcription/translation during long-term plasticity, surprisingly little has been elucidated on their relationship to the concrete implementation of long-lasting synaptic modifications. The evidence presented here suggests that STC may operate at least in part via two related yet distinct limbs of CaMK signaling: tag setting by CaMKII and activity-dependent gene transcription regulation by a CaMKK-dependent pathway. This new model nicely accounts for the interactive yet orthogonal (synapse-specific vs cell-wide) nature of tag setting and PRP synthesis, which might be coregulated in parallel via distinct pools of Ca^{2+}/CaM. However, the molecular basis of the tag–PRP interactions remains unclear. Better understanding of CaMKII dynamics (kinase activity and kinase content) and molecular dissection of the CaMKII-containing protein complexes at activated synapses will clearly be important steps toward solving this issue (Lisman et al., 2002; Yamauchi, 2005).

Because our data here establish the necessity for CaMKII activation to initiate the tag-setting process, one attractive idea is to consider that perhaps autophosphorylation of CaMKII itself might constitute the "tag" or be an integral part of it. However, independent studies have also shown evidence suggesting that pCaMKII signal may sometimes spread beyond the area of the originally stimulated synapses (Ouyang et al., 1997; Rose et al., 2009). The mechanistic basis for such potential loss of input specificity at the pCaMKII level remains unsolved. Additional studies are needed to resolve this apparent contradiction and pin down the molecular identity of the tag set in motion by CaMKII activation.

The wider implications of this work for the neurobiology of memory are of considerable interest. It provides a candidate mechanism for how inconsequential events (mimicked by weak stimulation in the protocols used here) may be remembered for much longer when they occur against the background of other surprising or emotionally significant events (mimicked by strong stimulation here), as occurs in flashbulb memory situations. Definitive evidence will require demonstration of STC *in vivo* and the creation of behavioral paradigms to investigate the transformation of short-term into long-term memory in complementary situations (Moncada and Viola, 2007).

References

Andersen P, Sundberg SH, Sveen O, Wigström H (1977) Specific long-lasting potentiation of synaptic transmission in hippocampal slices. Nature 266:736–737.

Bito H, Deisseroth K, Tsien RW (1996) CREB phosphorylation and dephosphorylation: a Ca^{2+}- and stimulus duration-dependent switch for hippocampal gene expression. Cell 87:1203–1214.

Bliss TV, Lomo T (1973) Long-lasting potentiation of synaptic transmission in the dentate area of the anaesthetized rabbit following stimulation of the perforant path. J Physiol 232:331–356.

Braun AP, Schulman H (1995) The multifunctional calcium/calmodulin-dependent protein kinase: from form to function. Annu Rev Physiol 57:417–445.

Erondu NE, Kennedy MB (1985) Regional distribution of type II Ca^{2+}/calmodulin-dependent protein kinase in rat brain. J Neurosci 5:3270–3277.

Fonseca R, Nägerl UV, Morris RG, Bonhoeffer T (2004) Competing for memory: hippocampal LTP under regimes of reduced protein synthesis. Neuron 44:1011–1020.

Fonseca R, Nägerl UV, Bonhoeffer T (2006) Neuronal activity determines the protein synthesis dependence of long-term potentiation. Nat Neurosci 9:478–480.

Frey U, Morris RGM (1997) Synaptic tagging and long-term potentiation. Nature 385:533–536.

Frey U, Morris RGM (1998a) Weak before strong: dissociating synaptic tagging and plasticity-factor accounts of late-LTP. Neuropharmacology 37:545–552.

Frey U, Morris RGM (1998b) Synaptic tagging: implications for late maintenance of hippocampal long-term potentiation. Trends Neurosci 21:181–188.

Frey U, Krug M, Reymann KG, Matthies H (1988) Anisomycin, an inhibitor of protein synthesis, blocks late phases of LTP phenomena in the hippocampal CA1 region in vitro. Brain Res 452:57–65.

Giese KP, Fedorov NB, Filipkowski RK, Silva AJ (1998) Autophosphorylation at Thr286 of the alpha calcium-calmodulin kinase II in LTP and learning. Science 279:870–873.

Hansel C, de Jeu M, Belmeguenai A, Houtman SH, Buitendijk GH, Andreev D, De Zeeuw CI, Elgersma Y (2006) alphaCaMKII Is essential for cerebellar LTD and motor learning. Neuron 51:835–843.

Hanson PI, Meyer T, Stryer L, Schulman H (1994) Dual role of calmodulin in autophosphorylation of multifunctional CaM kinase may underlie decoding of calcium signals. Neuron 12:943–956.

Ho N, Liauw JA, Blaeser F, Wei F, Hanissian S, Muglia LM, Wozniak DF, Nardi A, Arvin KL, Holtzman DM, Linden DJ, Zhuo M, Muglia LJ, Chatila TA (2000) Impaired synaptic plasticity and cAMP response element-binding protein activation in Ca^{2+}/calmodulin-dependent protein kinase type IV/Gr-deficient mice. J Neurosci 20:6459–6472.

Ho OH, Delgado JY, O'Dell TJ (2004) Phosphorylation of proteins involved in activity-dependent forms of synaptic plasticity is altered in hippocampal slices maintained in vitro. J Neurochem 91:1344–1357.

Ishida A, Kameshita I, Okuno S, Kitani T, Fujisawa H (1995) A novel highly specific and potent inhibitor of calmodulin-dependent protein kinase II. Biochem Biophys Res Commun 212:806–812.

Kang H, Sun LD, Atkins CM, Soderling TR, Wilson MA, Tonegawa S (2001) An important role of neural activity-dependent CaMKIV signaling in the consolidation of long-term memory. Cell 106:771–783.

Kawashima T, Okuno H, Nonaka M, Adachi-Morishima A, Kyo N, Okamura M, Takemoto-Kimura S, Worley PF, Bito H (2009) Synaptic activity-responsive element in the Arc/Arg3.1 promoter essential for synapse-to-nucleus signaling in activated neurons. Proc Natl Acad Sci U S A 106:316–321.

Krug M, Lössner B, Ott T (1984) Anisomycin blocks the late phase of long-term potentiation in the dentate gyrus of freely moving rats. Brain Res Bull 13:39–42.

Leutgeb JK, Frey JU, Behnisch T (2003) LTP in cultured hippocampal-entorhinal cortex slices from young adult (P25-30) rats. J Neurosci Methods 130:19–32.

Lisman J, Schulman H, Cline H (2002) The molecular basis of CaMKII function in synaptic and behavioural memory. Nat Rev Neurosci 3:175–190.

Lisman JE, Goldring MA (1988) Feasibility of long-term storage of graded information by the Ca^{2+}/calmodulin-dependent protein kinase molecules of the postsynaptic density. Proc Natl Acad Sci U S A 85:5320–5324.

Lisman JE, Zhabotinsky AM (2001) A model of synaptic memory: a CaMKII/PP1 switch that potentiates transmission by organizing an AMPA receptor anchoring assembly. Neuron 31:191–201.

Malenka RC, Kauer JA, Perkel DJ, Mauk MD, Kelly PT, Nicoll RA, Waxham MN (1989) An essential role for postsynaptic calmodulin and protein kinase activity in long-term potentiation. Nature 340:554–557.

Malinow R, Schulman H, Tsien RW (1989) Inhibition of postsynaptic PKC or CaMKII blocks induction but not expression of LTP. Science 245:862–866.

Martin KC, Casadio A, Zhu H, Yaping E, Rose JC, Chen M, Bailey CH, Kandel ER (1997) Synapse-specific, long-term facilitation of aplysia sensory to motor synapses: a function for local protein synthesis in memory storage. Cell 91:927–938.

Meyer T, Hanson PI, Stryer L, Schulman H (1992) Calmodulin trapping by calcium-calmodulin-dependent protein kinase. Science 256:1199–1202.

Miller P, Zhabotinsky AM, Lisman JE, Wang XJ (2005) The stability of a stochastic CaMKII switch: dependence on the number of enzyme molecules and protein turnover. PLoS Biol 3:e107.

Miller SG, Kennedy MB (1986) Regulation of brain type II Ca^{2+}/calmodulin-dependent protein kinase by autophosphorylation: a Ca^{2+}-triggered molecular switch. Cell 44:861–870.

Moncada D, Viola H (2007) Induction of long-term memory by exposure to novelty requires protein synthesis: evidence for a behavioral tagging. J Neurosci 27:7476–7481.

Navakkode S, Sajikumar S, Frey JU (2007) Synergistic requirements for the induction of dopaminergic D1/D5-receptor-mediated LTP in hippocampal slices of rat CA1 in vitro. Neuropharmacology 52:1547–1554.

O'Carroll CM, Morris RGM (2004) Heterosynaptic co-activation of glutamatergic and dopaminergic afferents is required to induce persistent long-term potentiation. Neuropharmacology 47:324–332.

Ouyang Y, Kantor D, Harris KM, Schuman EM, Kennedy MB (1997) Visualization of the distribution of autophosphorylated calcium/calmodulin-dependent protein kinase II after tetanic stimulation in the CA1 area of the hippocampus. J Neurosci 17:5416–5427.

Reymann KG, Frey JU (2007) The late maintenance of hippocampal LTP: requirements, phases, "synaptic tagging", "late-associativity" and implications. Neuropharmacology 52:24–40.

Rose J, Jin SX, Craig AM (2009) Heterosynaptic molecular dynamics: locally induced propagating synaptic accumulation of CaM kinase II. Neuron 61:351–358.

Sajikumar S, Navakkode S, Frey JU (2005) Protein synthesis-dependent long-term functional plasticity: methods and techniques. Curr Opin Neurobiol 15:607–613.

Sajikumar S, Navakkode S, Frey JU (2007) Identification of compartment- and process-specific molecules required for "synaptic tagging" during long-term potentiation and long-term depression in hippocampal CA1. J Neurosci 27:5068–5080.

Sajikumar S, Navakkode S, Frey JU (2008) Distinct single but not necessarily repeated tetanization is required to induce hippocampal late-LTP in the rat CA1. Learn Mem 15:46–49.

Sanhueza M, McIntyre CC, Lisman JE (2007) Reversal of synaptic memory by Ca^{2+}/calmodulin-dependent protein kinase II inhibitor. J Neurosci 27:5190–5199.

Schurr A, Reid KH, Tseng MT, Edmonds HL Jr, West CA, Rigor BM (1986) Effect of electrical stimulation on the viability of the hippocampal slice preparation. Brain Res Bull 16:299–301.

Schwartzkroin PA, Wester K (1975) Long-lasting facilitation of a synaptic potential following tetanization in the in vitro hippocampal slice. Brain Res 89:107–119.

Sumi M, Kiuchi K, Ishikawa T, Ishii A, Hagiwara M, Nagatsu T, Hidaka H (1991) The newly synthesized selective Ca^{2+}/calmodulin dependent protein kinase II inhibitor KN-93 reduces dopamine contents in PC12h cells. Biochem Biophys Res Commun 181:968–975.

Tokumitsu H, Inuzuka H, Ishikawa Y, Ikeda M, Saji I, Kobayashi R (2002) STO-609, a specific inhibitor of the Ca^{2+}/calmodulin-dependent protein kinase kinase. J Biol Chem 277:15813–15818.

Yamauchi T (2005) Neuronal Ca^{2+}/calmodulin-dependent protein kinase II—discovery, progress in a quarter of a century, and perspective: implication for learning and memory. Biol Pharm Bull 28:1342–1354.

Zhang YP, Holbro N, Oertner TG (2008) Optical induction of plasticity at single synapses reveals input-specific accumulation of αCaMKII. Proc Natl Acad Sci U S A 105:12039–12044.

Cellular/Molecular

Control of Cortical Axon Elongation by a GABA-Driven Ca^{2+}/Calmodulin-Dependent Protein Kinase Cascade

Natsumi Ageta-Ishihara,[1] Sayaka Takemoto-Kimura,[1] Mio Nonaka,[1] Aki Adachi-Morishima,[1] Kanzo Suzuki,[1] Satoshi Kamijo,[1] Hajime Fujii,[1] Tatsuo Mano,[1] Frank Blaeser,[2] Talal A. Chatila,[3] Hidenobu Mizuno,[4,5] Tomoo Hirano,[4,5] Yoshiaki Tagawa,[4,5] Hiroyuki Okuno,[1,5] and Haruhiko Bito[1,5]

[1]Department of Neurochemistry, Graduate School of Medicine, University of Tokyo, Tokyo 113-0033, Japan, [2]Institute of Transfusion Medicine, University Hospital Leipzig, 04129 Leipzig, Germany, [3]Division of Immunology, Allergy, and Rheumatology, Department of Pediatrics, David Geffen School of Medicine, University of California, Los Angeles, Los Angeles, California 90095-1752, [4]Department of Biophysics, Kyoto University Graduate School of Science, Kyoto 606-8502, Japan, and [5]Core Research for Evolutional Science and Technology, Japan Science and Technology Agency, Saitama 332-0012, Japan

Ca^{2+} signaling plays important roles during both axonal and dendritic growth. Yet whether and how Ca^{2+} rises may trigger and contribute to the development of long-range cortical connections remains mostly unknown. Here, we demonstrate that two separate limbs of the Ca^{2+}/calmodulin-dependent protein kinase kinase (CaMKK)–CaMKI cascades, CaMKK–CaMKIα and CaMKK–CaMKIγ, critically coordinate axonal and dendritic morphogenesis of cortical neurons, respectively. The axon-specific morphological phenotype required a diffuse cytoplasmic localization and a strikingly α-isoform-specific kinase activity of CaMKI. Unexpectedly, treatment with muscimol, a $GABA_A$ receptor agonist, selectively stimulated elongation of axons but not of dendrites, and the CaMKK–CaMKIα cascade critically mediated this axonogenic effect. Consistent with these findings, during early brain development, *in vivo* knockdown of CaMKIα significantly impaired the terminal axonal extension and thereby perturbed the refinement of the interhemispheric callosal projections into the contralateral cortices. Our findings thus indicate a novel role for the GABA-driven CaMKK–CaMKIα cascade as a mechanism critical for accurate cortical axon pathfinding, an essential process that may contribute to fine-tuning the formation of interhemispheric connectivity during the perinatal development of the CNS.

Introduction

The formation of cortical neural circuits requires precisely controlled development of axons and dendrites. Although the molecular mechanisms underlying axon guidance in the CNS have been intensively studied (Tessier-Lavigne and Goodman, 1996; Dickson, 2002), the intracellular signaling and cytoskeletal remodeling mechanisms implicated in the precise extension and targeting of axonal arbors still remain mostly unsolved.

Ca^{2+} plays a central role in the regulation of neuronal morphogenesis. It is believed that there is an elevated optimal range for the intracellular Ca^{2+} concentration that supports maximal neurite outgrowth in various types of neurons (Kater et al., 1988; Gomez and Zheng, 2006). Ca^{2+}/calmodulin-dependent protein kinases (CaMKs), a major Ca^{2+}-dependent kinase family, are good candidates as potential downstream effectors of calcium elevation in neurons (Soderling and Stull, 2001; Hudmon and Schulman, 2002). Although the essential role of CaMKII subfamily members in neuronal plasticity has been shown, much less is known about the function of the CaMKI/IV subfamily, which forms several distinct kinase cascades downstream of CaMK kinase α (CaMKKα) and/or CaMKKβ (Soderling, 1999; Hook and Means, 2001; Hudmon and Schulman, 2002; Bito and Takemoto-Kimura, 2003). The CaMKI family includes four isoforms: α (Nairn and Greengard, 1987), β/Pnck (Yokokura et al., 1997), γ/CL3 (Takemoto-Kimura et al., 2003), and δ/CKLiK (Ishikawa et al., 2003). Recently, a few reports from several laboratories, including ours, have started to suggest, *in vitro*, that CaMKI activity may participate in the regulation of neuronal morphology such as growth cone motility (Wayman et al., 2004), neurite outgrowth (Schmitt et al., 2004; Uboha et al., 2007), activity-dependent growth of dendrites (Wayman et al., 2006; Takemoto-Kimura et al., 2007), and stabilization of spines (Saneyoshi et al., 2008). However, evidence based on materials

Received June 25, 2009; revised Aug. 18, 2009; accepted Sept. 29, 2009.

This work was supported in part by grants-in-aid from the Ministry of Education, Culture, Sports, Science and Technology of Japan (S.T.-K., Y.T., T.H., H.O., H.B.) and the Ministry of Health, Labour and Welfare of Japan (H.B.), 21st Century Center of Excellence (COE) and Global COE Programmes (H.B.), by a grant from the National Institutes of Health (T.A.C.), and by awards from the Astellas Foundation for Research on Metabolic Disorders (H.B., S.T.-K.), the Naito Foundation (S.T.-K.), the Cell Science Research Foundation, the Takeda Foundation, and the Toray Science Foundation (H.B.). N.A.-I. and M.N. were predoctoral and postdoctoral fellows funded by Japan Society for the Promotion of Science, respectively. We thank all members of the Bito laboratory for support and discussion, T. Soderling and G. Wayman for constructive comments on a previous version of this work, and M. Kano for initially providing access to a validated working stock of muscimol. We are grateful to H. Tokumitsu (Kagawa University) for CaMKK-β WT and V269F cDNA; to J. Nabekura (National Institute for Physiological Sciences, Aichi, Japan) and K. Nakayama (Showa University, Tokyo, Japan) for a KCC2 plasmid; to R. Y. Tsien (Howard Hughes Medical Institute and University of California, San Diego, La Jolla, CA) for mRFP1 and mCherry cDNAs; and to K. Fukunaga and J. Kasahara (Tohoku University) for a rabbit anti-CaMKIα antibody. BDNF was supplied by Dainippon Sumitomo Pharma Co., Ltd. through the courtesy of C. Nakayama and T. Ishiyama. We are also indebted to assistance from K. Saiki, Y. Kondo, and T. Kinbara.

Correspondence should be addressed to Haruhiko Bito, Department of Neurochemistry, Graduate School of Medicine, University of Tokyo, 7-3-1 Hongo, Bunkyo-ku, Tokyo 113-0033, Japan. E-mail: hbito@m.u-tokyo.ac.jp.

N. Ageta-Ishihara's present address: Division of Biological Sciences, Graduate School of Science, Nagoya University, Furo-cho, Chikusa-ku, Nagoya 464-8602, Japan.

DOI:10.1523/JNEUROSCI.3018-09.2009

 0270-6474/09/2913720-10$15.00/0